Multinuclear Paramagnetic NMR Spectra and Solid State X-ray Crystallographic Characterization of Manganese(III) Schiff-Base Complexes

Yangzhen Ciringh,[†] Scott W. Gordon-Wylie,[†] Richard E. Norman,[‡] George R. Clark,[§] Susan T. Weintraub,[||] and Colin P. Horwitz*,[†]

Department of Chemistry, Carnegie Mellon University, Pittsburgh, Pennsylvania 15213, Department of Chemistry and Biochemistry, Duquesne University, Pittsburgh, Pennsylvania 15282, Department of Chemistry, The University of Auckland, Auckland, New Zealand, and Department of Biochemistry, The University of Texas Health Science Center, San Antonio, Texas 78284

Received June 17, 1997[⊗]

The ^{1}H NMR spectra of symmetrically substituted paramagnetic [(R,R′-SALOPHEN)Mn^{III}]$^+$ and [(R,R′-SALOPHEN)Mn^{III}]$_2$(μ-O) complexes (SALOPHEN is 1,3-bis(salicylideneamino)benzene) were obtained. All of the monomers and dimers yielded well-resolved but isotropically shifted ^{1}H NMR spectra. A diamagnetic suppression routine was applied to the ^{1}H NMR spectra that allowed observation of all rapidly relaxing resonances. The binding of axial ligands, acetate, methanol, water, and pyridine was also observable by ^{1}H NMR. Two X-ray crystal structures were obtained: [(3,3′-17-crown-6-SALOPHEN)Mn^{III}]·($CH_3C(O)O$)·$BaTf_2$·$2H_2O$, [**9b**]-OAc·$BaTf_2$·$2H_2O$, crystallized in the triclinic space group $P\bar{1}$; with a = 10.747(2) Å, b = 12.271(8) Å, c = 16.206(6) Å, α = 106.10(4)°, β = 103.07(2)°, γ = 106.06(3), and Z = 2, while [(3,3′,6,6′-$(CH_3)_4$-SALOPHEN)-Mn^{III}]PF_6·H_2O, [**6b**]PF_6·H_2O, crystallized in the monoclinic space group $P2_1/n$, with a = 12.465(1) Å, b = 13.366-(2) Å, c = 15.240(1) Å, β = 103.051(7)°, and Z = 2. [**9b**]OAc·$BaTf_2$·$2H_2O$ has the Mn(III) center ligated in the axial positions by one oxygen of the acetate group and an oxygen from one $SO_3CF_3^-$. The second oxygen of the acetate is bound to the Ba^{2+} residing in the crown ether. The water molecule in [**6b**]PF_6·H_2O is O-bound to the Mn(III) center and also hydrogen bonded to one of the fluorine atoms of the PF_6 counterion, O−F 3.01 Å. ^{1}H and ^{19}F NMR spectra revealed that the hydrogen bond in [**6b**]PF_6·H_2O was preserved in CD_3OD.

Introduction

Polymetallic coordination compounds of Mn(III) and Mn-(IV) containing bridging oxo ligands have been studied as structural and chemical models for the tetranuclear manganese site in the oxygen-evolving complex (OEC) of photosystem II (PSII) and the dinuclear site in manganese catalase[1−3] and also for their magnetic properties.[2,4] This has led to a tremendous amount of insight into the chemical and physical properties of oxo-bridged manganese cluster compounds. NMR spectroscopy is one technique that has not been applied extensively to Mn-(III) coordination complexes because they are almost always paramagnetic (S = 2), which complicates acquisition and interpretation of their NMR spectra. However, well-resolved, isotropically shifted ^{1}H NMR spectra of high-spin Mn(III) complexes can be obtained.[5−9] For example, high-quality ^{1}H NMR spectra were recently reported for some Mn(III) Schiff-base complexes possessing alkane backbones.[10−13] Chemical shift assignments were made for ligand hydrogens lying outside what is typically considered as the diamagnetic region (0−14 ppm) through systematic substitution of the ligand hydrogens. Two important observations from those studies are that (a) ligand geometry (e.g., planar *vs* twisted) markedly affected the chemical shift pattern for the ligand hydrogens[10] and (b) chemical reactions of paramagnetic Mn(III) complexes[13,14] can be followed by NMR spectroscopy.

We have been examining the reaction of O_2 with Mn(II) Schiff-base complexes **Ia**−**c** (R is an alkyl substituent) in nonaqueous solution.[15−18] The products isolated from these

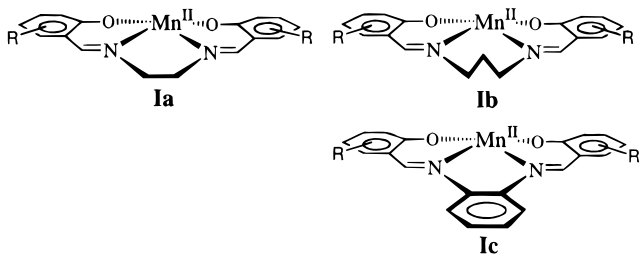

Ia **Ib** **Ic**

reactions include Mn(III) monomers, Mn^{IV}_2 bis(μ-oxo) dimers,

[†] Carnegie Mellon University.
[‡] Duquesne University.
[§] The University of Auckland.
[||] The University of Texas Health Science Center.
[⊗] Abstract published in *Advance ACS Abstracts,* September 15, 1997.

(1) Wieghardt, K. *Angew. Chem., Int. Ed. Engl.* **1989**, *28*, 1153.
(2) Manchanda, R.; Brudvig, G. W.; Crabtree, R. H. *Coord. Chem. Rev.* **1995**, *144*, 1.
(3) Larson, E. J.; Pecoraro, V. L. In *Introduction to Manganese Enzymes*; Larson, E. J., Pecoraro, V. L., Eds.; VCH Publishers: New York, 1992; p 1.
(4) Wemple, M. W.; Tsai, H.-L.; Wang, S.; Claude, J. P.; Streib, W. E.; Huffman, J. C.; Hendrickson, D. N.; Christou, G. *Inorg. Chem.* **1996**, *35*, 6437.
(5) Bertini, I.; Turano, P.; Vila, A. J. *Chem. Rev.* **1993**, *93*, 2833.
(6) La Mar, G. N. *NMR of Paramagnetic Molecules; Principles and Applications*; Academic Press: New York, 1973.
(7) La Mar, G. C.; Walker, F. A. *J. Am. Chem. Soc.* **1973**, *95*, 6950.
(8) La Mar, G. C.; Walker, F. A. *J. Am. Chem. Soc.* **1975**, *97*, 5103.
(9) LaMar, G. N.; Horrocks, W. D., Jr.; Holm, R. H. *NMR of Paramagnetic Molecules*; Academic Press: New York, 1973.
(10) Bonadies, J. A.; Kirk, M. L.; Lah, M. S.; Kessissoglou, D. P.; Hatfield, W. E.; Pecoraro, V. L. *Inorg. Chem.* **1989**, *28*, 2037.
(11) Gohdes, J. W.; Armstrong, W. H. *Inorg. Chem.* **1992**, *31*, 368.
(12) Li, X.; Pecoraro, V. L. *Inorg. Chem.* **1989**, *28*, 3403.
(13) Caudle, M. T.; Riggs-Gelasco, P.; Gelasco, A. K.; Penner-Hahn, J. E.; Pecoraro, V. L. *Inorg. Chem.* **1996**, *35*, 3577.
(14) Rogers, K. R.; Goff, H. M. *J. Am. Chem. Soc.* **1988**, *110*, 7049.
(15) Dailey, G. C.; Horwitz, C. P.; Lisek, C. A. *Inorg. Chem.* **1992**, *31*, 5325.
(16) Horwitz, C. P.; Ciringh, Y.; Liu, C.; Park, S. *Inorg. Chem.* **1993**, *32*, 5951.
(17) Horwitz, C. P.; Dailey, G. C. *Comments Inorg. Chem.* **1993**, *14*, 283.

S0020-1669(97)00747-7 CCC: $14.00

Scheme 1

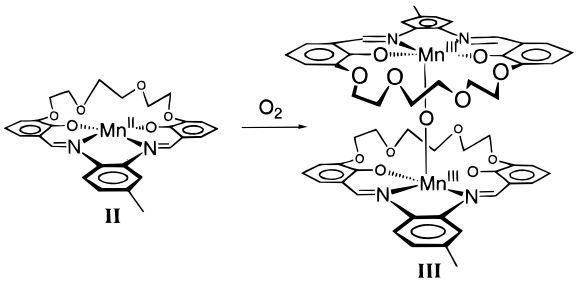

and Mn^{III}_2 μ-oxo dimers. The nature of the oxidized product depends both on the solvent used during the oxygenation[19] and on ligand backbone flexibility. Oxygenation in methanol yields cationic Mn(III) monomers while oxygenation in CH_3CN or CH_2Cl_2 using the same Mn(II) complex produces a neutral oxo-bridged dimer. Backbone flexibility also is important in determining which dimer forms because the ligand twists into a *cis*-β geometry in the bis(μ-oxo) dimer.[11,20] Thus, the Mn^{IV}_2 bis(μ-oxo) dimer is isolated when Mn(II) complexes with flexible ligand backbones, **Ia** or **Ib**, are oxidized.

We recently reported that oxygenation of 3,3′-17-crown-6-SAL-4-CH_3-(OPHEN)Mn^{II}, **II**, in CH_3CN produced a Mn^{III}_2 μ-oxo dimer, **III** (Scheme 1).[21] The crown ether groups on **III** incorporate alkali and alkaline earth cations. The cation-binding property of **III** is interesting because it allows one to begin probing the role that Ca^{2+}, an inorganic cofactor for the function of the OEC,[22] might play in the water oxidation process catalyzed by PSII.[23] Analogous chemistry has now been extended to the Mn^{IV}_2 bis(μ-oxo) dimers.[24,25] We found for **III** that large anodic potential shifts occurred for the $Mn^{III/II}_2$ couple upon cation incorporation and that the shifts were consistent with an electrostatic effect. For example, Ba^{2+} incorporation into **III** shifted the $Mn^{III/II}_2$ couple anodically by 300 mV when compared to the cation-free complex.

Electrochemical experiments on **III** revealed that the two metal centers were extremely weakly coupled despite being connected by the bridging oxo ligand. This weak coupling was manifested by the two Mn(III) centers having two reversible one electron reduction processes at nearly the same potential. In contrast, Mn^{III}_2 μ-oxo dimers having bridging groups such as acetate connecting the Mn(III) centers in addition to the oxo bridge, exhibit strongly coupled metal centers, and therefore have distinct mixed-valence redox states.[1] We have now prepared and characterized several Mn^{III}_2 μ-oxo dimers with SALOPHEN derivatives and have found that all show the same electron transfer characteristics as **III**. Unfortunately, single crystals suitable for X-ray crystallographic analysis have not yet been obtained for any of the derivatives, so a structurally based rationalization of the electron transfer properties is not yet possible.

As noted above, the chemical shift pattern in the ^1H NMR spectrum of the hydrogens on Schiff-base ligands depends on ligand geometry. This was of interest to us because we felt it might be useful to employ this information to distinguish and characterize those Mn(III) compounds for which we have been unable to obtain single-crystal X-ray crystallographic data. Furthermore, it was anticipated that the results of the NMR study would provide a means of determining if the oxo-bridged dimers have significantly different ligand geometries than their corresponding monomers, which might account for their unusual electron transfer properties.

Table 1. Ligands Used in This Study

	substituent						
complex[a]	3,3′	4,4′	5,5′	6,6′	7,7′	8,8′	9.9′
1	H	H	H	H	H	H	H
2	CH_3	H	H	H	H	H	H
3	H	OCH_3	H	H	H	H	H
4	H	H	OCH_3	H	H	H	H
5	$(CH_3)_3C$	H	CH_3	H	H	H	H
6	CH_3	H	H	CH_3	H	H	H
7	H	H	H	H	H	H	CH_3
8	$(CH_3)_3C$	H	CH_3	H	D	H	H
9[b]	$C_3H_6O_2$	H	H	H	H	H	H

[a] The designators **a**, **b**, and **c** in the text refer to Mn(II) complexes, Mn(III) monomer complexes, and μ-oxo-bridged Mn(III) dimers, respectively. [b] This substituent is a polyether chain linking the 3 and 3′ positions like the one shown in Scheme 1.

The principal focus here is the characterization by paramagnetic ^1H NMR spectroscopy of the Mn(III) monomers and Mn^{III}_2 μ-oxo dimers with SALOPHEN type ligands, **IV** (Table 1).

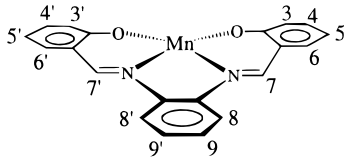

IV

Some compounds in this study were also examined by paramagnetic ^{19}F and ^{23}Na spectroscopy. An application of the standard inversion recovery technique[26] was used to gather the ^1H NMR data. The method described in the Experimental Section provided a means of enhancing the paramagnetic signals while decreasing those arising from residual hydrogens of the deuterated solvents and any hydrogen-containing diamagnetic impurities, primarily water, in the solvents. This allowed us to observe all of the ligand hydrogens and also to probe axial ligation properties of Mn(III). More importantly, the data acquisition method should be applicable to other paramagnetic transition metal complexes having electronic properties similar to those found for Mn(III) and thus could provide a new method for examining chemical and physical properties of these molecules.

We show in this report that NMR spectroscopy is extremely useful for characterizing and distinguishing Mn(III) monomers from oxo-bridged dimers and that the planar ligand geometry of the monomer likely is conserved in the dimer. In addition, we found that multinuclear NMR spectroscopy permits one to readily observe the binding of acetate, methanol, water, and pyridine to Mn(III) centers in the monomers. Coordination of water and pyridine to Mn(III) in the dimers also is observable. Finally, paramagnetic ^{19}F NMR data reveal that the hydrogen bond between an axially bound water molecule and the PF_6 counteranion observed in the solid state for one of the monomer complexes is preserved in CD_3OD.

(18) Horwitz, C. P.; Winslow, P. J.; Warden, J. T.; Lisek, C. A. *Inorg. Chem.* **1993**, *32*, 82.
(19) Gallo, E.; Solari, E.; Re, N.; Floriani, C.; Chiesi-Villa, A.; Rizzoli, C. *Angew. Chem., Int. Ed. Engl.* **1996**, *35*, 1981.
(20) Larson, E. J.; Las, M. S.; Li, X.; A., B. J.; Pecoraro, V. L. *Inorg. Chem.* **1992**, *31*, 373.
(21) Horwitz, C. P.; Ciringh, Y. *Inorg. Chim. Acta* **1994**, *225*, 191.
(22) Yocum, C. F. In *The Calcium and Chloride Requirements for Photosynthetic Water Oxidation*; Yocum, C. F., Ed.; VCH Publishers, Inc.: New York, 1992; p 71.
(23) Ghanotakis, D. F.; Yocum, C. F. *Annu. Rev. Plant Physiol. Plant Mol. Biol.* **1990**, *255*, 41.
(24) Horwitz, C. P.; Warden, J. T.; Weintraub, J. T. *Inorg. Chim. Acta* **1996**, *246*, 311.
(25) Ciringh, Y.; Horwitz, C. P. Unpublished results.
(26) Harris, R. K. *Nuclear Magnetic Resonance Spectroscopy*; Longman Scientific & Technical: Essex, 1986.

Experimental Section

Physical Measurements. ^{1}H NMR spectra were measured at 300 MHz on an IBM NR/300 FT-NMR spectrometer. FTIR spectra (KBr disks) were taken on a Mattson 5000 FTIR spectrometer while UV/vis spectra were obtained using a Hewlett-Packard HP8452A spectrophotometer. Elemental analyses were performed by Midwest Microlab, Indianapolis, IN. Electrochemical measurements were performed using a Princeton Applied Research Model 273 potentiostat/galvanostat with current voltage curves recorded on a Graphtec Model WX1200 X-Y recorder. The supporting electrolyte was 0.1 M [*n*-Bu_4N][PF_6] (TBAPF_6, Fluka puriss). Cyclic voltammograms were performed under N_2 in a three-compartment cell using a glassy carbon disk working electrode, a Pt wire counter electrode, and a sodium chloride saturated calomel electrode (SSCE) reference electrode. Electrospray ionization mass spectrometry (ESI-MS) was performed at University of Texas Health Science Center at San Antonio. ESI mass spectra were acquired on a Finnigan MAT SSQ700 mass spectrometer fitted with an Analytica of Branford electrospray ionization interface. Electrospray voltages of 2400−3400 V were utilized. Samples were dissolved in either CH_3CN or CH_2Cl_2 at concentrations of approximately 10 pmol/μL and were introduced into the ESI interface by direct infusion at a flow rate of 1 μL/min. Spectral averaging for 1−2 min was employed prior to data acquisition.

Diamagnetic Suppression Routine for ^{1}H NMR Data. An inversion recovery pulse sequence, $\pi-\tau-\pi/2-$acquire, was applied. A series of spectra was obtained where the variable delay time, τ, was chosen to be in the range of approximately 0.1−5 times the T_1 value for the paramagnetically shifted hydrogens (T_{1p}). At short τ ($\tau_1 \sim 0.1T_{1p}$), the signals arising from the paramagnetic and the diamagnetic (solvent and water) portions were inverted. A longer τ, $\tau_2 = (3-5)T_{1p}$, was then chosen such that the paramagnetic signals were fully relaxed, i.e., close to the maximum positive intensity, while the diamagnetic signals remained inverted. It was necessary to choose $\tau_2 - \tau_1$ to be small compared to the T_1 values for the diamagnetic protons (T_{1d}) so that the net change in the diamagnetic signal intensity was minimal. Subtraction of the spectra at the chosen τ_2 and τ_1 values then capitalized on the differential relaxation effects between the paramagnetic and diamagnetic signals and resulted in an enhancement of the paramagnetic signals and suppression of the diamagnetic ones. Typical operating parameters were as follows: spectrometer frequency (SF), 300.135 MHz; data block size (SI), 16K; resolution (RES), 3.59 Hz/pt; acqusition time (AQ), 0.279 s; and relaxation delay (RD), 0 s.

^{19}F and ^{23}Na NMR Data. ^{19}F and ^{23}Na NMR data were obtained using parameters standard for the instrument (^{19}F, SF 282.386 MHz, SI 32K, RES 7.629 Hz/pt, and AQ 0.131 s; ^{23}Na, SF 79.391 MHz, SI 8K, RES 20.345 Hz/pt, and AQ 0.030s), and in both cases the RD was set to 0. Wide sweep widths were used in survey spectra so that signals of reasonable intensity did not go unobserved.

Materials. The reagent grade chemicals 2-*tert*-butyl-4-methylphenol, $SnCl_4$, $(H_2CO)_n$, NaH, triethylene glycol ditosylate, 1,2-diaminobenzene, 2,3-dihydroxybenzaldehyde, 3,4-diaminotoluene, 2,6-lutidine, 2-methylphenol, 2,4-dimethylphenol, 2-hydroxy-4-methoxybenzaldehyde, 2-hydroxy-5-methoxybenzaldehyde, $Mn(CH_3C(O)O)_2\cdot 4H_2O$, and $Ba(SO_3CF_3)_2$ ($BaTf_2$) were used as received from Aldrich. The $[SO_3CF_3]^-$ salts of Na^+ (NaTf), K^+ (KTf), and Ca^{2+} ($CaTf_2$), as well as [Cp_2Fe][PF_6], were prepared by methods described in the literature.[27,28] $(D_2CO)_n$ (99% d_2) CD_2Cl_2, CD_3CN, C_5D_5N, and CD_3OD were obtained from Cambridge Isotope Laboratories and used without further purification. Cp_2Co (Strem) was purified by sublimation prior to use. The ligand 3,3′-17-crown-6-SALOPHEN-H_2 was prepared by the method of van Staveren et al.[27] and its purity determined by ^{1}H NMR spectroscopy. The solvents CH_3CN, CH_2Cl_2, DMF, and CH_3OH were purified by standard methods[29] while dry ether (Aldrich) was used as received. Air sensitive compounds were prepared under nitrogen using Schlenk techniques and stored in an Ar-filled glovebox (Vacuum Atmospheres).

Aldehyde Syntheses. Salicylaldehyde derivatives not commercially available were prepared by the method of Casiraghi et al.,[30] but the purification procedures were modified as follows: 2-hydroxy-3-methylbenzaldehyde was purified by vacuum distillation; 2-hydroxy-3-*tert*-butyl-5-methylbenzaldehyde was purified by sublimation under vacuum; 2-hydroxy-3,6-dimethylbenzaldehyde was purified by column chromatography on silica gel using 80% hexanes/20% ether as eluant, and the first band is the desired product. The 2-hydroxy-3-*tert*-butyl-5-methylbenzaldehyde-*d* was prepared using CD_2O and purified by vacuum sublimation. Product purities were determined by ^{1}H NMR spectroscopy.

Metal Complex Syntheses. (R,R′-SALOPHEN)Mn^{II} (R = R′ = H, 1a; 3-CH_3, 2a; 4-CH_3O, 3a; 5-CH_3O, 4a; 3-*t*-Bu-5-CH_3, 5a; 3,6-$(CH_3)_2$, 6a). The same general procedures were followed for the preparation of all of the Mn(II) complexes, so only the synthesis of **2a** is described. The solids 2-hydroxy-3-methylbenzaldehyde (556 mg, 2 mmol) and 1,2-diaminobenzene (108 mg, 1 mmol) were combined in a Schlenk flask and then dissolved in methanol (20 mL), resulting in the formation of a yellow solution, which was refluxed under N_2 for about 30 min. The solution was cooled to 20 °C, KOH (112 mg, 2 mmol) in deoxygenated methanol (10 mL) was added, and the solution was stirred for 10 min. $Mn(CH_3C(O)O)_2\cdot 4H_2O$ (245 mg, 1 mmol) ($MnCl_2$ can be used in place of the acetate) dissolved in deoxygenated methanol was added to the solution of the deprotonated ligand, which caused the solution to immediately become deep red; in most cases a yellowish brown precipitate formed . The mixture was refluxed for 1 h to ensure complete reaction. After cooling to 20 °C, the solid was recovered by filtration, washed with 20 mL of deoxygenated water, and dried under vacuum.

[(R,R′-SALOPHEN)Mn^{III}]PF_6 (R = R′ = H, [1b]PF_6; 3-CH_3, [2b]PF_6; 4-CH_3O, [3b]PF_6; 5-CH_3O, [4b]PF_6; 3-*t*-Bu-5-CH_3, [5b]PF_6; 3,6-$(CH_3)_2$, [6b]PF_6). The same procedures were used to prepare all of these Mn(III) complexes, so only the synthesis of [**2b**]PF_6 is described. Compound **2a** (50 mg, 0.13 mmol) was slurried in 10 mL of O_2-free CH_3OH, and then O_2 was bubbled through the solution for about 15 min, producing a dark brown solution. A 4-fold molar excess of NH_4PF_6 was added as a solid to the solution, and this mixture was stirred until all of the solid was consumed and a dark brown homogeneous solution remained. The methanol was removed *in vacuo*, and the solid product was washed with copious quantities of H_2O. After the solid was redissolved in dry CH_3CN and the solution was dried over Na_2SO_4, the solvent volume was reduced to about 5 mL, and a solid precipitated on addition of dry ether. The solid was recovered by filtration and dried under vacuum at approximately 100 °C for 10 h. Yield: 80−85%. Anal. Calcd (found): for $C_{20}H_{14}N_2O_2MnPF_6$, [**1b**]PF_6, C 46.69 (46.97), H 2.75 (2.87), N 5.45 (5.77); $C_{22}H_{18}N_2\cdot O_2MnPF_6\cdot {}^1/_3CH_3CN$, [**2b**]$PF_6$; C 48.17 (48.09), H 3.43 (3.60), N 5.42 (5.11); $C_{22}H_{18}N_2O_2MnPF_6$, [**3b**]PF_6, C 45.99 (45.86), H 3.16 (3.3), N 4.88 (5.05); $C_{22}H_{18}N_2O_2MnPF_6\cdot {}^1/_2H_2O$, [**4b**]$PF_6$, C 45.28 (45.09), H 3.28 (3.31), N 4.8 (5.09); $C_{30}H_{34}N_2O_2MnPF_6\cdot {}^1/_2CH_3CN\cdot {}^1/_2H_2O$, [**5b**]$PF_6$, C 54.41 (54.51), H 5.38 (5.66), N 5.12(5.42); $C_{22}H_{18}N_2\,O_2MnPF_6\cdot {}^1/_3H_2O$, [**6b**]$PF_6$, C 49.99 (50.04), H 3.97 (4.22), N 4.86 (4.77). UV/vis λ/nm ($\epsilon \times 10^3$ M^{-1} cm^{-1}): for [**2b**]PF_6 (CH_3OH) 246 (43.2), 306 (23.2), 350 (31.4), 444 (9.4); [**3b**]PF_6 (CH_3CN) 256 (32.3), 314(sh) (22), 352 (29.5), 394 (sh) (17.2), 432 (sh) (14); [**5b**]PF_6 (CH_3CN) 254 (31.3), 308 (20.5), 342 (21.4), 358 (22.5), 474 (6.1).

[(SAL-3,4-$(CH_3)_2$-OPHEN)Mn^{III}]PF_6 ([7b]PF_6). The procedure used to prepare this compound was the same as the one for the [(R,R′-SALOPHEN)Mn^{III}]PF_6 complexes, except that 4,5-dimethyl-1,2-phenylenediamine was used in place of 1,2-diaminobenzene. Anal. Calcd (found) for $C_{22}H_{18}N_2O_2MnPF_6\cdot {}^1/_2CH_3CN$, [**7b**]$PF_6$: C 49.06 (48.93), H 3.49 (3.56), N 6.22 (6.08). UV/vis in CH_3OH, λ/nm ($\epsilon \times 10^3$ M^{-1} cm^{-1}): 250 (40.5), 298 (21.6), 344 (26.5), 432 (10.9).

[(3,3′-(*t*-Bu)$_2$-5,5′-$(CH_3)_2$-SALOPHEN-d_2)Mn^{III}]PF_6 ([8b]PF_6). 2-Hydroxy-3-*tert*-butyl-5-methylbenzaldehyde-*d* (192 mg, 1.0 mmol) and 1,2-diaminobenzene (54 mg, 0.5 mmol) were dissolved in CH_3OD (5 mL, 99% D), and the resulting yellow solution was refluxed under N_2 for about 30 min. After cooling to room temperature, KOD in 1 mL of CH_3OD (prepared by dissolving KOH (56.1 mg, 1.0 mmol)

(27) van Staveren, C. J.; van Eerden, J.; M van Veggel, F. C. J.; Harkema, S.; Reinhoudt, D. N. *J. Am. Chem. Soc.* **1988**, *110*, 4994.
(28) Yang, E. S.; Chan, M. S.; Wahl, A. C. *J. Phys. Chem.* **1975**, *79*, 2049.
(29) Perrin, D. D.; Armarego, W. L. F. *Purification of Laboratory Chemicals*, 3rd ed.; Pergamon Press: Oxford, England, 1988.
(30) Casiragi, G.; Casnati, G.; Puglia, G.; Startori, G.; Terenghi, G. *J. Chem. Soc., Perkin Trans 1* **1980**, 1862.

in CH_3OD) was added to the solution of the ligand, followed by stirring for 10 min. Exchangeable hydrogens on $Mn(CH_3C(O)O)_2 \cdot 4H_2O$ were exchanged with deuterium by dissolving the Mn(II) salt in CH_3OD and then removing the CH_3OD *in vacuo*. A CH_3OD (1 mL) solution of the deuterium-exchanged Mn(II) salt (122.5 mg, 0.5 mmol) was then added to the solution containing the deprotonated ligand. The mixture was refluxed for 1 h to ensure complete reaction and then cooled to room temperature, and then O_2 was bubbled through the solution. After the reaction was judged to be complete as evidenced by a homogeneous solution (30−60 min), a 4-fold molar excess of solid NH_4PF_6 was added. Purification was accomplished by the procedure described above for **5b**. ESI-MS: $[\mathbf{8b}]^+$ *m/z* 511.4.

[(R,R′-SALOPHEN)Mn^{III}]$_2$(μ-oxo) (R = R′ = H, 1c; 3-CH_3, 2c; 4-CH_3O, 3c; 5-CH_3O, 4c; 3-*t*-Bu-5-CH_3, 5c; 3,6-$(CH_3)_2$, 6c). The same basic procedures were used to prepare all of the Mn^{III}_2 μ-oxo dimers, so only the one for **1c** is described. Compound **1a** (50 mg, 0.14 mmol) was loaded in a flask in the glovebox and dissolved in CH_2Cl_2 (25 mL), and the flask sealed with a rubber septum. After the flask was removed from the glovebox, O_2 was allowed to flow over the top of the solution slowly, causing the golden yellow slurry to become a homogeneous red brown solution. The solvent volume was reduced to 5 mL, and pentane was added to precipitate a brown powder. The solid was recovered by filtration through a medium-porosity glass frit and dried under vacuum. Anal. Calcd (found) for $C_{40}H_{28}N_4O_5Mn_2 \cdot 2CH_2Cl_2$, **1c**: C 58.71 (58.61), H 3.61 (3.39), N 6.68 (6.44). ESI-MS: $[\mathbf{1c}H]^+$ *m/z* 755. Anal. Calcd (found) for $C_{60}H_{68}N_4O_5Mn_2 \cdot 3H_2O$, **5c**: C 66.15 (66.26), H 6.85 (6.48), N 5.15 (4.85). ESI-MS: $[\mathbf{5c}H]^+$ *m/z* 1035.4. UV/vis (CH_2Cl_2) λ/nm ($\epsilon \times 10^3$ M^{-1} cm^{-1}): 306 (29.9), 344 (30.5), 360 (30.0), 486 (13.7).

[(3,3′-(*t*-Bu)$_2$-5,5′-$(CH_3)_2$-SALOPHEN-d_2)Mn^{III}]$_2$(μ-O) (8c). The Mn(II) starting material **8a** was synthesized as described for compounds **1a**−**6a** except that CH_3OD was used during the Schiff-base condensation and metalation reactions. After isolation, **8a** was oxidized and isolated by a procedure analogous to the one described for the synthesis of **5c**. ESI-MS: $[\mathbf{8c}H]^+$ *m/z* 1039.4.

(3,3′-17-Crown-6-SALOPHEN)Mn^{II}·$CH_3C(O)OH$ (9a·HOAc). The ligand H_2-3,3′-17-crown-6-SALOPHEN (150 mg, 0.32 mmol) was dissolved in dried, deaerated CH_3OH (15 mL) and refluxed under N_2 for 20 min to remove traces of O_2 from the solution. After cooling to 20 °C, $Mn(CH_3C(O)O)_2 \cdot 4H_2O$ (80 mg, 0.32 mmol) dissolved in 10 mL of CH_3OH was added to the ligand, producing a golden yellow solution. The solution was refluxed under N_2 for 30−45 min to assure complete reaction. No precipitate appeared at 20 °C, so the solvent was removed *in vacuo* leaving a golden yellow solid, which was washed with copious quantities of H_2O. After drying, the solid was redissolved in CH_3CN the solution filtered, and then the solvent removed *in vacuo*. The golden yellow solid was dried at 50 °C for 2 h. Yield: 80−85%. Anal. Calcd (found) for $C_{26}H_{24}O_6N_2Mn \cdot CH_3C(O)OH$: C 58.44 (58.48), H 4.9 (5.11), N 4.87 (5.34).

[(3,3′-17-Crown-6-SALOPHEN)Mn^{III}]·PF_6 ([9b]PF_6). This compound was prepared by a method described for the analog with a 4-methyl-1,2-diaminobenzene backbone.[21] Yield: 85−90%. Anal. Calcd (found) for $C_{26}H_{24}N_2O_6MnPF_6 \cdot 3H_2O$: C 45.41(45.22), H 3.96 (3.73), N 4.08 (4.13). UV/vis (CH_3CN) λ/nm (ϵ x 10^3 M^{-1} cm^{-1}): 246 (73.5), 314 (39.6), 370 (41.8), 474 (8.0).

[(3,3′-17-Crown-6-SALOPHEN)Mn^{III}][$CH_3C(O)O$] ([9b]OAc). A sample of **9a·HOAc** (50 mg, 0.097 mmol) was loaded in a Schlenk flask in an inert atmosphere glovebox and dissolved in deoxygenated CH_3CN (20 mL). The flask was removed from the glovebox, and then O_2 was slowly passed over the solution by means of a T-tube fitted onto the Schlenk flask. Oxygenation was carried out for approximately 16 h, during which time the solution changed from golden yellow to brown and a brown precipitate formed. The solid was recovered by filtration through a medium-porosity glass frit, washed with CH_3CN, and dried under vacuum. Yield 80−85%.

[(3,3′-17-Crown-6-SALOPHEN)Mn^{III}]·OAc·$BaTf_2$ ([9b]·OAc·$BaTf_2$). A sample of [**9b**]OAc (50 mg, 0.048 mmol) was combined with $BaTf_2$ (42.6 mg, 0.096 mmol) in 10 mL of CH_3CN, and the mixture was stirred until all of the solid dissolved. A deep red solution formed. The solvent volume was reduced to about 5 mL, and then Et_2O was allowed to slowly diffuse into the CH_3CN solution, resulting in the precipitation of a red brown crystalline solid, which was recovered by filtration and dried under vacuum. This crystalline material was used for a single-crystal X-ray structural determination. Anal. Calcd (found) for $C_{28}H_{27}N_2O_8Mn \cdot Ba(CF_3SO_3)_2$: C 35.65 (35.11), H 2.69 (2.80), N 2.77 (2.66). ESI-MS: *m/z* 861 $[[\mathbf{9b}]OAc \cdot Ba(CF_3SO_3)]^+$, *m/z* 356 $[[\mathbf{9b}]OAc \cdot Ba]^{2+}$, *m/z* 951 $[[\mathbf{9b}] \cdot Ba(CF_3SO_3)_2]^+$.

Table 2. Crystallographic Data for [**9b**]OAc·$BaTf_2$·$2H_2O$ and [**6b**]PF_6·H_2O

	[**9b**]OAc·$BaTf_2$·$2H_2O$	[**6b**]PF_6·H_2O
formula	$C_{30}H_{31}BaF_6MnN_2O_{16}S_2$	$C_{20}H_{24}O_3N_2MnPF_6$
formula weight	1045.97	588.37
cryst dimens (mm)	0.35 × 0.30 × 0.11	0.40 × 0.15 × 0.10
space group	$P\bar{1}$	$P2_1/n$
a (Å)	10.747(2)	12.465(1)
b (Å)	12.271(8)	13.366(2)
c (Å)	16.206(6)	15.240(1)
α (deg)	106.10(4)	
β (deg)	103.07(2)	103.051(7)
γ (deg)	106.06(3)	
V (Å^3)	1864.0(14)	2473.5(4)
d_{calc} (g cm^{-3})	1.864	1.580
Z	2	4
radiation, *λ* (Å)	Mo Kα, 0.710 69	Mo Kα, 0.710 69
T (°C)	−80	21
R^a	0.0352	0.065
wR_2[b]	0.0878	
R_w[c]		0.052

[a] $R_1 = \Sigma||F_o| - |F_c||/\Sigma|F_o|$. [b] $wR_2 = [\Sigma[w(F_o^2 - F_c^2)^2/\Sigma[w(F_o^2)^2]]^{1/2}$. [c] $R_w = [(\Sigma w(|F_o| - |F_c|)^2/\Sigma wF_o^2)]^{1/2}$.

Crystallographic Data Collection and Refinement of the Structures. (a) [9b]OAc·$BaTf_2$·$2H_2O$. Crystals of [**9b**]OAc·$BaTf_2$·$2H_2O$ were obtained by the slow diffusion of Et_2O into an CH_3CN solution of [**9b**]OAc·$BaTf_2$ in air. X-ray diffraction measurements were made on an Enraf-Nonius CAD-4 diffractometer with graphite-monochromated Mo Kα radiation. Cell constants, Table 2, and an orientation matrix were obtained from a least-squares refinement by using the setting angles of 25 carefully centered reflections in the range 19.5° < 2θ < 25.4°. The unit cell is triclinic ($P\bar{1}$; No. 2) with cell constants as given in Table 2. Intensity data were collected at 193 ± 2 K using the $\omega-2\theta$ scan technique to a maximum $2\theta_{max} = 54°$ for $\pm h, +k, \pm l$. Of the 7434 reflections collected, 7120 were unique ($R_{int} = 0.021$). Data were corrected for Lorentz and polarization effects, and for absorption by the empirical ψ scan method.[31]

The structure was solved by direct methods using SHELXS.[32] The non-hydrogen atoms were refined anisotropically. All hydrogen atoms could be located in the difference electron density maps and were refined satisfactorily with individual isotropic temperature factors. The final cycles of full-matrix least-squares refinement on F^2 were based on 7119 reflections and 656 parameters and converged (largest parameter shift was 0.021 times its esd) with $R_1 = 0.0352$ and $wR_2 = 0.0878$ [$I > 2\sigma(I)$], Table 2. The refinement program employed was SHELXL93.[33] Atomic scattering factors for neutral atoms were taken from *International Tables for X-ray Crystallography*.[34]

(b) [6b]PF_6·H_2O. Crystals of [**6b**]PF_6·H_2O were obtained by the slow diffusion of Et_2O into an CH_3CN solution of [**6b**]PF_6 in air. All measurements were made on a Rigaku AFC7R diffractometer with graphite-monochromated Mo Kα radiation. Cell constants, Table 2, and an orientation matrix for data collection, which was obtained from a least-squares refinement using the setting angles of 25 carefully centered reflections in the range 16.81° < 2θ < 22.37°, corresponded to the monoclinic space group $P2_1/n$ (No. 14). The data were collected at 21 °C using the $\omega-2\theta$ scan technique to $2\theta_{max} = 45.0°$. ω scans of several intense reflections that were made prior to data collection had an average width at half-height of 0.25°, with a takeoff angle of 6.0°. Scans of (1.21 + 0.35 tanθ)° were made at 16.0°/min (in omega). Weak

(31) North, A. C.; Phillips, D. C.; Matthews, F. S. *Acta Crystsllogr.* **1968**, *A24*, 351.
(32) Sheldrick, G. M. *Crystallographic Computing 3*; Sheldrick, G. M., Ed.; Oxford University Press: Oxford, England, 1985, p 175.
(33) Sheldrick, G. M., SHELXL93.
(34) Ibers, J. A.; Hamilton, W. C. *International Tables for X-ray Crystallography*; Kynoch Press: Birmingham, England, 1974; Vol. IV.

reflections ($I < 10.0\sigma(I)$) were rescanned (four scans maximum), and the counts were accumulated to ensure good counting statistics. Stationary background counts were recorded on each side of the reflection. The ratio of peak counting time to background counting time was 2:1. Of the 3591 reflections collected, 3413 were unique ($R_{int} = 0.054$). The intensities of three representative reflections measured after every 150 reflections. Over the course of data collection, the standards increased by 0.6%. A linear correction factor was applied to the data to account for this phenomenon. The data were corrected for Lorentz and polarization effects.

The structure was solved by direct methods[35] and expanded using Fourier techniques.[36] Non-hydrogen atoms were refined anisotropically. Hydrogen atoms were included but not refined. The final cycle of full-matrix least-squares refinement was based on 1624 observed reflections ($I > 2.00\sigma(I)$) and 334 variable parameters and converged (largest parameter shift was 0.01 times its esd) with $R = 0.065$ and $R_w = 0.052$, Table 2. The standard deviation of an observation of unit weight was 2.76. The weighting scheme was based on counting statistics and included a factor ($\rho = 0.004$) to downweight the intense reflections. The maximum and minimum peaks on the final difference Fourier map corresponded to 0.54 and -0.38 $e^-/Å^3$, respectively. Neutral atom scattering factors[37] and anomalous dispersion terms were included.[38] All calculations were performed using teXsan[39] from Molecular Structure Corporation.

Results and Discussion

Syntheses of Mn(II) Monomers. The ligands used in this study (Table 1) were prepared by condensation of 1,2-phenylenediamine or 4,5-dimethyl-1,2-phenylenediamine with the appropriate aldehyde in CH_3OH under an inert atmosphere. In general, the ligands were not isolated but were metalated *in situ* using either $Mn(CH_3C(O)O)_2 \cdot 4H_2O$ or $MnCl_2$. KOH in CH_3OH was added prior to the Mn(II) treatment to facilitate the metalation process. Most of the Mn(II) complexes, which are yellow-brown to brown except for **9a**, which is orange, precipitated from the CH_3OH solution. The solids were recovered by filtration, washed with copious quantities of deoxygenated water to remove residual salts, and then dried *in vacuo* (80−100 °C) for 3−5 h. For those Mn(II) compounds that were soluble in CH_3OH, the solvent was stripped off *in vacuo* and the solid washed with deoxygenated water and then dried *in vacuo*. Acceptable combustion analytical data were obtained for all of the Mn(II) complexes.

Deprotonation of the ligand by KOH was not employed during the synthesis of **9a** to avoid incorporation of K^+ in the crown ether. As a consequence, the product precipitated with one acetic acid molecule per Mn(II) even though it was washed with water and dried under vacuum for an extended period of time. This compound is referred to as **9a**·HOAc. The presence of the acetate ion was confirmed by synthesizing the deuterated analog of **9a**·HOAc using $Mn(CD_3C(O)O)_2$, which was prepared by refluxing $Mn(CH_3C(O)O)_2$ in $CD_3C(O)OD$ overnight followed by removal of the acid under vacuum, and then drying the solid for 3 h at 80 °C under vacuum. The IR spectrum of **9a**·$CD_3C(O)OD$ displayed absorption bands in the 2265 and 2105 cm^{-1} regions from C−D stretching vibrations. The corresponding bands in **9a**·HOAc are masked by other ligand C-H vibrations. As discussed below, under some synthetic conditions used to prepare the corresponding Mn(III) monomer from **9a**·HOAc, the acetate ion from the acetic acid solvate binds to the Mn(III) center.

Syntheses of Mn(III) Monomers. Two principal methods were used to prepare the Mn(III) monomers. In the first, a Mn(II) complex was oxidized in CH_3OH by bubbling O_2 through the solution (this method is referred to as the CH_3OH/O_2 method; eq 1). The resulting Mn(III) product, which was brown for [**1b**]$^+$, [**2b**]$^+$, [**4b**]$^+$, [**5b**]$^+$, and [**6b**]$^+$ and dark blue for [**3b**]$^+$ and [**7b**]$^+$, was isolated as a PF_6^- salt. Paramagnetic ^1H NMR results, presented below, revealed that complexes prepared in this manner likely have CH_3OH as an axial ligand. The second method involved oxidation of a Mn(II) complex under N_2 or Ar with $[Cp_2Fe]^+$ in CH_3CN ($CH_3CN/[Cp_2Fe]^+$ method; eq 2) followed by isolation as the PF_6^- salt. These compounds appear to have CH_3CN as the axial ligand. Compounds prepared by either synthetic method and "dried" *in vacuo* at 60−80 °C exhibited identical combustion analytical data (<0.4% error for each element analyzed), indicating loss of the axial ligand during the drying process. We refer to compounds dried at 60−80 °C as "dried monomers" while those only briefly exposed to vacuum at 20 °C are designated as "solvated monomers". A dried monomer is less soluble in CH_3CN than a solvated one, but both are freely soluble in CH_3OH. The ^1H NMR spectrum of a dried monomer in CD_3CN (presented below) is suggestive of loss of the axial CH_3OH or CH_3CN with an accompanying dimerization or oligomerization of the monomers for a portion of the sample.

$$(CH_3OH)(L)Mn^{II} + O_2 \xrightarrow{CH_3OH} [(CH_3OH)_x(L)Mn^{III}]^+ \xrightarrow[\text{vacuum}]{\Delta} [(L)Mn^{III}]^+ \quad (1)$$

$$(CH_3CN)(L)Mn^{II} + Cp_2Fe^+ \xrightarrow{CH_3CN} [(CH_3OH)_x(L)Mn^{III}]^+ \xrightarrow[\text{vacuum}]{\Delta} [(L)Mn^{III}]^+ \quad (2)$$

L = R,R′-SALOPHEN; $x = 1$ or 2

Oxygenation of **9a**·HOAc in CH_3OH followed by the addition of NH_4PF_6 produced the Mn(III) monomer, [**9b**]PF_6. In contrast, oxygenation of **9a**·HOAc in CH_3CN produced [**9b**]OAc as a red-brown precipitate. The low solubility of [**9b**]OAc in CH_3CN may be due to formation of a polymeric material in which acetate groups bridge the Mn(III) centers.[10,40−42] As discussed below, oxygenation of all of the other Mn(II) complexes in CH_3CN resulted in the formation of Mn^{III}_2 μ-oxo dimers. Apparently the acetic acid present in **9a**·HOAc either intercepted intermediates during μ-oxo dimer formation or cleaved the dimer after it formed.

The addition of Na^+, K^+, Ca^{2+}, or Ba^{2+} ($[SO_3CF_3]^-$ salts) to a slurry of [**9b**]OAc in CH_3CN resulted in the formation of a homogeneous red-brown solution within approximately 5−10 min. Single crystals of [**9b**]OAc containing Ba^{2+} were isolated from the slow diffusion of Et_2O into a CH_3CN solution of the compound in air. The result of the X-ray analysis is shown in Figure 1a. Crystallographic data for [**9b**]OAc·$BaTf_2 \cdot 2H_2O$ are given in Table 2, and selected bond distances and angles are

(35) Altomare, A.; Cascarano, M.; Giacovazzo, C.; Guagliardi, A.; Burla, M. C.; Polidori, G.; Camalli, M. *J. Appl. Crystallogr.* **1994**, *27*, 435.
(36) Beurskens, P. T.; Admiraal, G.; Beurskens, G.; Bosman, W. P.; Garcia-Granda, S.; Gould, R. O.; Smits, J. M. M.; Smykalla, C. The DIRDIF program system. Technical Report of the Crystallography Laboratory, University of Nijmegen: Nijmegen, The Netherlands, 1992.
(37) Cromer, D. T.; Waber, J. T. *International Tables for X-ray Crystallography;* Kynoch Press: Birmingham, England, 1974; Vol. IV, Table 2.2 A.
(38) Ibers, J. A.; Hamilton, W. C. *Acta Crystallogr.* **1964**, *17*, 781.
(39) teXsan, Crystal Structure Analysis Package.
(40) Aurangazeb, N.; Hulme, C. E.; McAuliffe, A. A.; Pritchard, R. G.; Watkinson, M.; Bermejo, M. R.; Sousa, A. *J. Chem. Soc., Chem. Commun.* **1994**, 2193.
(41) Aurangazeb, N.; Hulme, C. E.; McAuliffe, A. A.; Pritchard, R. G.; Watkinson, M.; Garcia-Deibe, A.; Bermejo, M. R.; Sousa, A. *J. Chem. Soc., Chem. Commun.* **1992**, 1524.
(42) Davies, J. E.; Gatehouse, B. M.; Murray, K. S. *J. Chem. Soc., Dalton Trans.* **1973**, 2523.

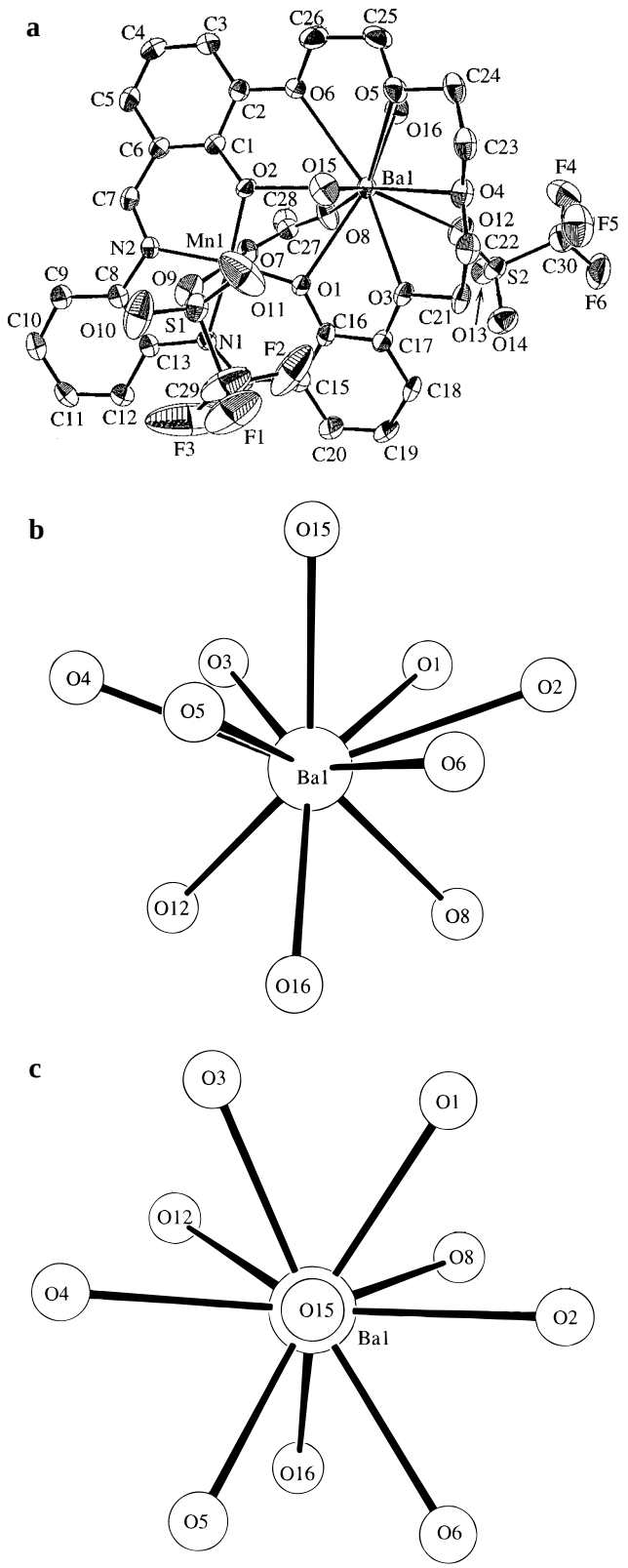

Figure 1. (a) ORTEP diagram and atom-labeling scheme of [**9b**]OAc·$BaTf_2$·$2H_2O$ with hydrogen atoms omitted and thermal ellipsoids at the 50% probability level (in this view O11 obscures Mn1). (b) View of the 1:6:3 coordination at Ba^{2+}. (c) View down the local C_3 axis at Ba^{2+}.

found in Table 3. Mn1 adopts a pseudo-octahedral geometry with the equatorial plane consisting of two imine nitrogens and two phenolate oxygens of the Schiff-base ligand. An oxygen from one triflate group and an oxygen from the acetate are the axial ligands. The ^{1}H NMR spectrum of [**9b**]OAc·$BaTf_2$·$2H_2O$, which is described below, reveals that the Mn(III) center is ligated by acetate in CD_3OD. The Mn−N and Mn−O distances to the Schiff-base ligand are similar to those found in other Schiff-base complexes.[42−47] Not unexpectedly, the Mn−O acetate distance, Mn1−O7 2.107(3) Å, is significantly shorter than the Mn−O triflate length, Mn1−O9 2.489(4) Å. The O7−Mn1−O9 angle is 168.21(11)°.

Table 3. Selected Bond Lengths (Å) and Angles (deg) for [**9b**]OAc·$BaTf_2$·$2H_2O$

Ba1−O16	2.691(4)	Mn1−O1	1.867(3)
Ba1−O8	2.732(3)	Mn1−O2	1.877(3)
Ba1−O15	2.767(4)	Mn1−N1	1.969(3)
Ba1−O1	2.786(3)	Mn1−N2	1.978(3)
Ba1−O5	2.791(3)	Mn1−O7	2.107(3)
Ba1−O3	2.817(3)	Mn1−O9	2.489(4)
Ba1−O2	2.863(3)	S1−O9	1.435(3)
Ba1−O4	2.863(3)	S2−O12	1.445(3)
Ba1−O12	2.884(3)	O7−C27	1.268(5)
Ba1−O6	2.917(3)	O8−C27	1.234(5)
Ba1−Mn1	3.741(2)		
O1−Mn1−O2	90.71(12)	O1−Mn1−O9	87.42(12)
O1−Mn1−N1	92.59(13)	O2−Mn1−O9	94.98(13)
O2−Mn1−N1	175.21(13)	N1−Mn1−O9	81.70(13)
O1−Mn1−N2	168.58(13)	N2−Mn1−O9	81.54(12)
O2−Mn1−N2	93.18(13)	O7−Mn1−O9	168.21(11)
N1−Mn1−N2	82.94(13)	C27−O7−Mn1	128.2(3)
O1−Mn1−O7	100.27(12)	C27−O8−Ba1	140.9(3)
O2−Mn1−O7	93.85(13)	S1−O9−Mn1	150.9(2)
N1−Mn1−O7	88.99(13)	S2−O12−Ba1	159.2(2)
N2−Mn1−O7	90.19(12)		

The coordination environment around the Ba^{2+} is novel (Figure 1b,c). The cation is coordinated by 10 oxygens: four from the crown ether, two from the H_2O molecules, two from the Schiff-base phenolate groups, one from the triflate group not bound to manganese, and one from the acetate. Except for the Ba1−O16 distance (2.691(4) Å), the Ba^{2+}−O distances (2.767(4)−2.917(3) Å) are within the range predicted[48] and found[49] for barium in a crown ether type environment. There is no obvious reason for the Ba1−O16 distance to be significantly shorter than the Ba1−O15 distance (2.767(4) Å) since both oxygens belong to H_2O molecules bound to Ba^{2+} and neither is involved in an H-bonding interaction with a neighboring complex. The arrangement of the ligating oxygens is best described as possessing C_{3v} local symmetry, with one oxygen (O15) (and the Ba^{2+}) on the C_3 axis, six oxygens in a hexagon above the Ba^{2+}, and three oxygens below the Ba^{2+} in a staggered arrangement with respect to the hexagon. The coordination polyhedron, thus, consists of a hexagonal pyramid with its six triangular faces at the "top", and a 3-fold alternation of triangular and trapezoidal faces downward to a triangle at the bottom. A more graphical description is a hexagonal pyramid on a triangular base. This 1:6:3 coordination geometry has not been seen previously. Other workers have categorized 10-coordination environments and, by energy minimization calculations, have deduced that six structures are possible.[50−52] They have

(43) Ashmawy, F. M.; Beagly, B.; McAuliffe, C. A.; Parish, R. V.; Pritchard, R. G. *J. Chem. Soc., Chem. Commun.* **1990**, 936.
(44) Gohdes, J. W.; Armstrong, W. H. *Inorg. Chem.* **1988**, *27*, 1841.
(45) Matsumoto, N.; Takemoto, N.; Ohyosi, A.; Okawa, H. *Bull. Chem. Soc. Jpn.* **1988**, *61*, 2984.
(46) Pecoraro, V. L.; Butler, W. M. *Acta Crystallogr.* **1986**, *C42*, 1151.
(47) Horwitz, C. P.; Dailey, G. C.; Tham, F. S. *Acta Crystallogr.* **1995**, *C51*, 815.
(48) Hay, B. P.; Rustad, J. R. *J. Am. Chem. Soc.* **1994**, *116*, 6316.
(49) Costes, J.-P.; Laurent, J.-P.; Chabert, P.; Commenges, G.; Dahan, F. *Inorg. Chem.* **1997**, *36*, 656.
(50) Favas, M. C.; Kepert, D. L. *Prog. Inorg. Chem.* **1981**, *28*, 309.
(51) Robertson, B. E. *Inorg. Chem.* **1977**, *16*, 2735.
(52) Lin, Y. C.; Williams, D. E. *Can. J. Chem.* **1972**, *51*, 312.

found that the bicapped square antiprism, the tetracapped trigonal prism, and the tetradecahedron are more stable than the pentagonal antiprism, the pentagonal prism, and the bicapped square prism. Thus, the coordination geometry observed here is not one of the predicted ones.

Synthesis of Mn^{III}_2 μ-Oxo Dimers. The Mn^{III}_2 μ-oxo dimers were prepared by oxygenation of the corresponding Mn(II) complexes in CH_3CN or CH_2Cl_2 (eq 3). We found that it was important to carry out the oxygenation slowly (24−72 h) because, otherwise, the sample could be contaminated with other oxo-bridged dimers. This slow oxidation was achieved by passing O_2 over an unstirred solution of the monomer. The ^{1}H NMR data for these compounds, described below, indicate that water is an axial ligand for the dimers; the water likely comes from trace water present in the solvents used during oxygenation.

$$(L)(L')Mn^{II} + O_2 \xrightarrow[\text{trace } H_2O]{CH_3CN \text{ or } CH_2Cl_2} [(H_2O)(L)Mn^{III}]_2(\mu\text{-}O) \quad (3)$$

L′ is CH_3CN or CH_3OH; L is a Schiff-base ligand

Paramagnetic NMR Spectroscopy. The observation of signals from paramagnetic molecules by ^{1}H NMR spectroscopy is not as straightforward as for diamagnetic species, but paramagnetic NMR spectroscopy is becoming an important tool for characterizing a number of transition metal complexes.[5,10,53] We found that, in order to obtain high-quality spectra of the Mn(III) Schiff-base complexes studied here, it was key that the intensity of the resonances arising from residual protons in the deuterated solvents as well as any ^{1}H NMR active impurities in the solvents, typically water, be diminished. These kinds of resonances are referred to here as diamagnetic signals. An application of the inversion recovery pulse sequence was used to perform the diamagnetic suppression. Specific experimental parameters used for collecting the data are given in the Experimental Section. Typical suppression factors for the diamagnetic signals were 5:1 to 10:1 while paramagnetic signals were enhanced by approximately 2:1. Although the overall effect of the suppression routine may appear to be fairly modest compared to more sophisticated pulse sequences, the experiment is easily performed and instrument setup parameters are straightforward. We have found that even paramagnetic peaks that are overlapped by diamagnetic peaks can be resolved by this approach because of the inherently different relaxation rates of the paramagnetic and diamagnetic resonances.

Sample preparation was important for achieving high-quality spectra. High concentrations of complex were used where possible (approximately 20 mg/mL of solvent) in order to decrease the total data acquisition time. Typically, monomers were dissolved in CH_3OD or CD_3OD prior to spectral acquisition to exchange CH_3OH, CH_3CN, or H_2O, the CH_3OD or CD_3OD was removed *in vacuo*, and then the sample was dissolved in the solvent of choice. This procedure could not be applied to the Mn^{III}_2 μ-oxo dimers because they decomposed in methanol. The dimers were dried at approximately 50 °C *in vacuo* prior to dissolution.

$[LMn^{III}]^+$ Monomers. The ^{1}H NMR spectra obtained for $[\mathbf{1b}]^+$ as a solvated monomer in CD_3OD, before and after application of the diamagnetic suppression routine, are shown in Figure 2 traces a and b, respectively. A total of seven resonances are expected for $[\mathbf{1b}]^+$ assuming C_{2v} symmetry, and seven are observed (Figure 2b). The resonance at −387 ppm is extremely broad and weak. Clear observation of the upfield resonance required a 10-fold longer acquisition time as compared to the remainder of the spectrum. The signal intensity of the upfield resonance has been enhanced 10-fold relative to the other resonances in Figure 2b and smoothed for purposes of clarity. The six resonances lying outside the diamagnetic region (0−14 ppm) are observed in both spectra, but the resonance at 1.8 ppm is clearly visible only after application of the diamagnetic suppression routine. The resonance at 1.8 ppm is masked in Figure 2a by the resonance arising from CH_3CN that was introduced during the synthesis of $[\mathbf{1b}]^+$ (see below). When pyridine-d_5 (py-*d*) was used as the solvent, the resonance at 1.8 ppm was still observed, so this signal is not an artifact of the spectral subtraction routine.

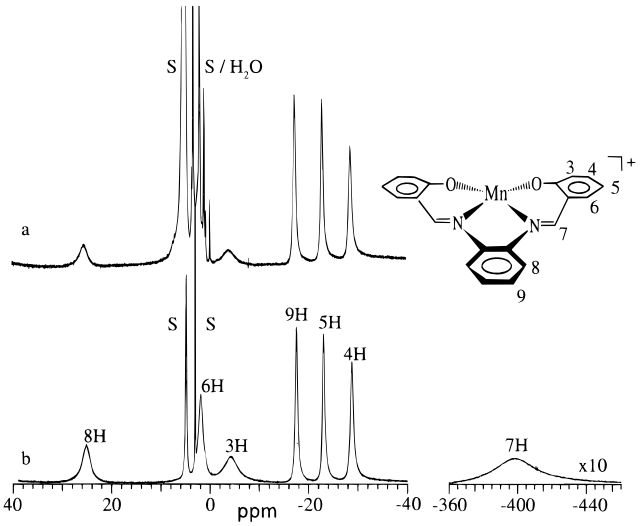

Figure 2. ^{1}H NMR spectra of a solvated sample of compound $[\mathbf{1b}]^+$ in CD_3OD: (a) before and (b) after application of the diamagnetic suppression routine.

It has been shown for Mn(III) Schiff-base complexes that the contact term which occurs through the phenol oxygens and imine groups accounts for most of the chemical shift.[54] The alternation in upfield/downfield resonances that one might expect as the aromatic rings of the ligand arms are traversed is not observed in the R,R′-SALOPHEN complexes because of the competing chemical shift determining pathways. However, since there is only one delocalization mechanism for the aromatic backbone, the resonance for either 8H or 9H should be in the upfield region and the other in the downfield region.

It was possible to determine the chemical shift assignments for all of the resonances observed in $[\mathbf{1b}]^+$ *via* a systematic substitution of the ligand hydrogens (Table 1). The matrix generated by the substitutions (Figure S1, Supporting Information) was used in providing the assignments indicated on Figure 2b. Given in Table 4 are the measured chemical shifts for the hydrogens on all of the complexes; T_{1p} values for some complexes are also included. The imine hydrogens (7H) of $[\mathbf{8b}]^+$ were selectively deuterated in order to show that 7H gave rise to the most upfield resonance. Synthesis of the deuterated ligand was straightforward as $(CD_2O)_n$ (99% d) could be used in place of $(CH_2O)_n$ in the aldehyde synthesis (see Experimental Section). It was necessary to perform the Schiff-base condensation and metalation reactions in CH_3OD to ensure that no loss of the deuterium label occurred. The compound having a CH_3 group on the 7-position also was prepared, but that substitution appeared to distort the ligand from planarity, thus affecting all of the resonance positions in this molecule.

We attempted to determine the T_{1p} value for 7H in $[\mathbf{1b}]^+$, but its extremely rapid relaxation rate only allowed us to

(53) Bertini, I.; Luchinat, C. *NMR of Paramagnetic Molecules in Biological Systems*; B. Cummings: Menlo Park, CA, 1986.

(54) Bonadies, J. A.; Maroney, M. J.; Pecoraro, V. L. *Inorg. Chem.* **1989**, *28*, 2044.

Table 4. Paramagnetic ^{1}H NMR Chemical Shifts, T_1 Values, and Electrochemical Data

complex	δ/ppm (T_1/ms) 3H	4H	5H	6H	7H	8H	9H	substituent: δ/ppm	C*H*$_3$ of bound OAc$^-$	bound H_2O	NMR solvent	E°/mV[a]
[**1b**]$^+$	−4.2 (0.43)	−28.9 (2.6)	−23.0 (3.1)	1.8 (0.8)	−398 (<0.4)	25.0 (0.65)	−17.6 (3.1)				CD_3OD	−20
[**2b**]$^+$		−34.5 (2.58)	−22.3 (3.73)	1.6	*b*	24.7	−17.6 (3.37)	3-CH_3: 19.5			CD_3OD	−36
[**3b**]$^+$	−10.6		−17.5	2.3	*b*	26.1	−16.4	4-CH_3O: 7.6			CD_3OD	−65
[**4b**]$^+$	−1.9	−21.8		1.3	*b*	24.0	−18.0	5-CH_3O: 5.3			CD_3OD	−78
[**5b**]$^+$		−29.6		2.8	−387	26.6	−17.7	3-*t*-Bu: 25.2 5-CH_3: 6.3			CD_3OD	−165
[**6b**]$^+$		−38.9	−20.2		*b*	25.2	−16.6	3-CH_3: 18.4 6-CH_3: 5.9			CD_3OD	−105
[**6b**]$^+$·CH_3OH		−38.9	−23.1		*b*	26.0	−17.0	3-CH_3: 21.8 6-CH_3: 6.8		12.7[c]	CD_3CN	
[**6b**]$^+$·CH_3CN		−39.0	−24.2		*b*	25.9	−17.1	3-CH_3: 22.9 6-CH_3: 7.1			CD_3CN	
[**6b**]PF_6·H_2O		−39.4	−20.3		*b*	25.9	−16.6	3-CH_3: 18.4 6-CH_3: 5.9		2.1	CD_3OD	
[**7b**]$^+$	−4.7	−27.4	−23.6	2.8	*b*	25.0		9-CH_3: 6.3			CD_3OD	−74
[**8b**]$^+$		−38.9	−20.2			25.2	−16.6	3-*t*-Bu: 6.3 5-CH_3: 25.2 7-D			CD_3OD	
[**9b**]PF_6		−34.7 (0.8)	−24.3 (2.3)	−1.5 (0.9)	*b*	23.9 (0.5)	−19.4 (1.9)				CD_3CN	−17
[**9b**]$^+$·Na^+ [d]		−33.2	−23.6	−3.0	*b*	25.2	−17.9			18	CD_3CN	
[**9b**]$^+$·K^+ [d]	(2.1)	−33.7 (2.5)	−24.6 (0.7)	−1.83	*b* (0.5)	25.2 (2.2)	−19.1			15	CD_3CN	19
[**9b**]$^+$·Ca^{2+} [d]		−29.1	−19.7	−7.4	*b*	25.9	−17.5			28	CD_3CN	
[**9b**]$^+$· Ba^{2+} [d]		−30.0 (1.6)	−21.8 (2.0)	−3.3 (0.9)	*b*	26.1 (0.4)	−19.3 (1.7)			17	CD_3CN	215
[**9b**]OAc·Na^+ [e]		−25.2	−17.7	−2.0	*b*	26.6	−13.8		39.1		CD_3CN	25
[**9b**]OAc· K^+ [e]		−26.9 (2.1)	−21.7 (2.5)	7.2 (0.7)	*b*	25.6 (0.5)	−15.0 (2.2)		41.3		CD_3CN	0
[**9b**]OAc·Ca^{2+} [e]		−25.7	−15.1	−5.7	*b*	26.0	−15.1		33.5		CD_3CN	240
[**9b**]OAc· $BaTf_2$·$2H_2O$[f]		−27.0 (2.3)	−20.1 (2.3)	−1.4 (0.5)	*b*	25.5 (0.6)	−16.9 (2.1)		36.1 (0.7)		CD_3CN	200
1c	31.6	−28.5	−22.9	−13.9	−354	23.6	−21.1			44.7	C_5D_5N[g]	
1c	40.5	−35.1	−26.1	−11.1	−348	25.2	−23.5			51.4	CD_2Cl_2	−130[h]
2c	23.9		−16.2	2.5	*b*	24.7	−14.3	3-CH_3		43.8	C_5D_5N[g]	
3c	11.7	−16		16.7	*b*	30	−7.2	4-CH_3O: 7.5		48.4	CD_2Cl_2	−215
5c		−21.2		14	−345	29.2	−9.2	3-t-Bu: 34 5-CH_3: 8.6		45.9	CD_2Cl_2	−270[h]
6c		−25	−20.3		*b*	24	−15.4	3-CH_3; 6-CH_3		44	C_5D_5N[g]	

[a] 0.1 M (*n*-Bu_4N)PF_6/CH_3CN; *E vs* SSCE. [b] Not measured. [c] C*H*$_3$ of bound CH_3OH. [d] Prepared *in situ* by the reaction of [**9b**]PF_6 with M^{n+} ($SO_3CF_3^-$ salt). [e] Prepared *in situ* by the reaction of [**9b**]OAc with M^{n+} ($SO_3CF_3^-$ salt). [f] Sample used for crystallographic analysis. [g] Spectrum obtained within 1 h of dissolution in py. [h] 0.1 M (*n*-Bu_4N)PF_6/CH_2Cl_2; *E vs* SSCE.

estimate that T_{1p} was less than 0.4 ms. This value corresponds to the most rapid T_{1p} measured for the Mn(III) monomer compounds in this study. Since 7H is in close proximity to the Mn(III) center and a conjugation pathway exists through the sp^2-hybridized imine group, both dipolar and scalar coupling mechanisms likely serve to very efficiently relax 7H. Owing to the long acquisition times required to observe 7H, no attempt was made to observe this resonance in all of the other compounds prepared in this study.

The spectrum of [**1b**]$^+$ as a dried monomer dissolved in CD_3CN is shown in Figure 3. In CD_3OD, the spectrum is identical to the one in Figure 2b. It is evident that, even though there are more resonances for the dried monomer than for the solvated monomer, the intense resonances in the spectrum have the same chemical shifts as those found for the solvated monomer. Similar increases in the number of resonances were recorded for all of the other dried monomers. As discussed below, the chemical shifts for the ligand hydrogens on monomers having CH_3OH, CH_3CN, or H_2O as axial ligands are not strongly influenced by the type of axial ligand. Therefore, the "new" resonances are not due to simply changing axial ligation.

It is likely that the new resonances arise from formation of dimers, **V**, of the Mn(III) monomers: trimers, tetramers, and other oligomers also are viable species that could give rise to the new resonances. Anion coordination to Mn(III) does not occur, as evidenced by the fact that vibrational bands of the anions in the FT-IR spectra of solvated and dried monomers are the same. As noted above, combustion analytical data reveal that a dried monomer loses its axial ligands. In order for Mn-

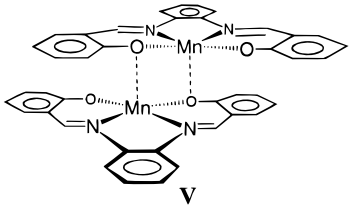

V

(III) to satisfy its requirement for axial ligands, a likely scenario is that a phenol oxygen from a nearby Mn(III) complex occupies an axial site. This type of interaction is observed in Cu, V, and Fe[55−57] Schiff-base chemistry, and we report here an example of such a dimer pair in the solid state (see Figure 8b). It appears that CD_3CN is not as strongly coordinating as CD_3-

(55) Hall, D.; Waters, T. N. *J. Chem. Soc.* **1960**, 2644.
(56) Gerloch, M.; Lewis, J.; Mabbs, F. E.; Richards, A. *Nature* **1966**, 809.
(57) Yamamoto, K.; Oyaizu, K.; Tsudhida, E. *J. Am. Chem. Soc.* **1996**, *118*, 12665.

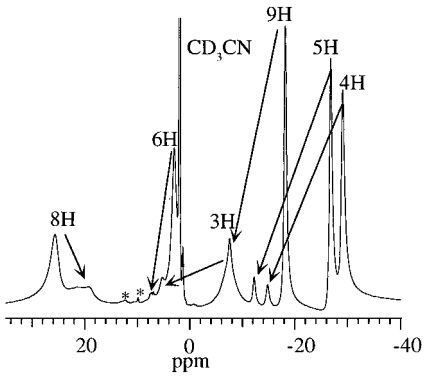

Figure 3. ^{1}H NMR spectrum of a dried sample of compound [**1b**]$^+$ in CD_3CN with diamagnetic suppression applied. Arrows indicate tentative resonance assignments for the dried monomer as derived from the solvated monomer spectrum. The resonance marked 3H is a composite of 3H and 9H in the dried monomer sample. An asterisk (*) indicates an impurity in the sample or solvent.

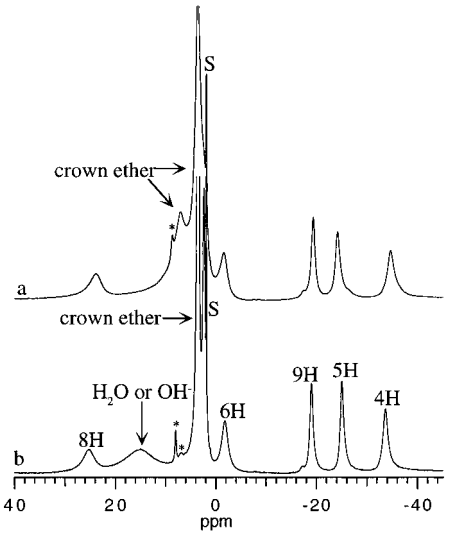

Figure 4. ^{1}H NMR spectra of a solvated sample of compound [**9b**]PF_6 in CD_3CN with diamagnetic suppression applied (a) before and (b) after the addition of 1 molar equiv of hydrated KSO_3CF_3. An asterisk (*) indicates an impurity in the sample or solvent.

OD and does not break up all of the dimers/oligomers formed during the drying process. The dimerization/oligomerization may occur for all or just a fraction of the complexes in a given sample; we do observe that the relative ratio of dried monomer to solvated monomer resonances depends on the length of the drying process and the ligand substitution. If the dimer/oligomer hypothesis is correct, then the close proximity of one or more $S = 2$ Mn(III) centers to the ligand hydrogens on a nearby Mn(III) complex could account for the shifts observed in the resonance positions. Tentative assignments for the new resonances are given in Figure 3. However, as some of the intensities were extremely weak, particularly those for 3H and 6H in [**1b**]$^+$, it is difficult to unambiguously assign all of the resonances.

Crown Ether Complex. The chemical shift assignments in the spectrum of [(3,3′-17-crown-6-SALOPHEN)Mn^{III}]PF_6, [**9b**]PF_6, taken in CD_3CN are based on the results from the solvated [(R,R′-SALOPHEN)Mn^{III}]PF_6 monomers discussed above as the pattern of three far-upfield resonances and one downfield resonance observed for [**1b**]$^+$ is preserved in [**9b**]PF_6 (Figure 4a and Table 4) (we did not attempt to locate 7H for [**1b**]$^+$ or its salt-containing derivatives). Two signals which are broad compared to solvent peaks but sharp compared to the paramagnetic signals appear in the diamagnetic region, and these are assigned to the $-CH_2-$ groups of the crown ether. Dried samples of [**9b**]PF_6 showed an increase in the number of resonances like the dried form of [**1b**]$^+$, but no obvious changes occurred for the crown ether portion of the molecule.

Cation-containing complexes of [**9b**]PF_6 were prepared *in situ* for ^{1}H NMR measurements by adding 1 equiv of a salt such as KTf to [**9b**]PF_6 in CD_3CN (Figure 4b and Table 4). Cation incorporation into **[9b]**$^+$ caused the resonance at 8 ppm to sharpen and shift upfield to 1.6 ppm. Similar effects occurred for the other crown ether resonance upon cation incorporation, but the upfield shift was from 2.1 to 1.9 ppm. All other signals from the ligand showed little change in their chemical shifts. The T_{1p} values for most of the hydrogens of the salt-containing complexes, [**9b**]$^+\cdot M^{n+}$, are close to those measured for [**9b**]PF_6 itself with the notable exception being 4H; because 4H is closest to the crown ether, its environment appears to be the most affected by the cation and any solvent molecules that might be bound to it. A new resonance from a water molecule or hydroxide ion bound to Mn(III) also appeared at 15 ppm following cation incorporation (see below). Since only the two resonances associated with the crown ether change significantly upon cation incorporation, this is strong evidence for cation insertion into the crown ether cavity. This same conclusion was deduced from electrochemical measurements on these (Table 4) and related compounds.[21]

We believe that the broad resonance at 15 ppm in Figure 4b arises from H_2O or OH^- bound to Mn(III) for the following reasons: (i) the resonance was present only when the compound was prepared using KTf that had not been rigorously dried; similar behavior was observed for the other salt-containing compounds (Table 4); (ii) this signal was lost upon the addition of D_2O; (iii) the chemical shift of the resonance was sensitive to the amount of water in solution; it shifted upfield, i.e., in the direction of free water, as the water concentration increased; and (iv) the very rapid T_{1p} value ($\sim$1 ms) supports binding to the Mn(III) center rather than to the cation in the crown ether. It is not possible to distinguish H_2O from OH^- with our current experiments; however, since a bound OH^- would reduce the overall charge on the complex following cation incorporation, at this time we favor hydroxide binding to the Mn(III) center.

The propensity of the [**9b**]$^+\cdot M^{n+}$ type complexes to bind water to Mn(III) suggests that the presence of the M^{n+} cation increases the Lewis acidity of the Mn(III) center and enhances its water/hydroxide binding properties. While monomers like [**9b**]$^+\cdot M^{n+}$ are structurally unrelated to PSII, the enhanced affinity of Mn(III) for water that results from having a cation within 3.6 Å of the metal center[27] leads us to suggest that the Ca^{2+} cation, which might be as close as 3.3 Å to the Mn_4 core of the OEC, may fill a similar role in the functioning enzyme.

The ^{23}Na NMR spectrum of [**9b**]$^+\cdot Na^+$ provided interesting information regarding cation insertion into the crown ether. As a reference we assigned NaTf in CD_3CN to 0 ppm. The chemical shift for NaTf in 18-crown-6/CD_3CN is -8.3 ppm, shifting slightly upfield upon the addition of water. The spectrum of a dried monomer of [**9b**]$^+\cdot Na^+$ in CH_3CN has two relatively broad resonances: an intense signal at 12 ppm, which is assigned to Na^+ in the crown ether of the monomer, and a smaller one at 421 ppm, which is assigned to Na^+ in the crown ether portion of the dimer/oligomer (Figure 5a). The 421 ppm resonance is lost upon the addition of water or methanol to the CD_3CN solution (Figure 5b); recall that methanol can be used to dissociate other dried monomers. Since both resonances are in different spectral regions than "free" Na^+ or Na^+ in 18-crown-6 in CD_3CN, this supports the binding of sodium by the crown ether in **[9b]**$^+$. Furthermore, the broadness of the

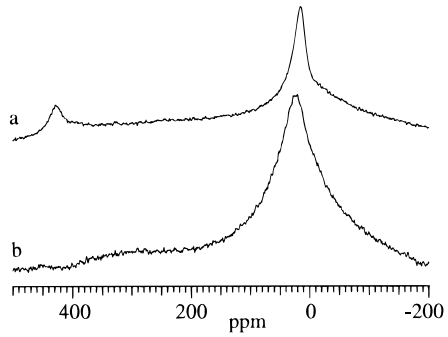

Figure 5. ^{23}Na spectra of a dried sample of [**9b**]PF_6 in CD_3CN containing 1 molar equiv of $NaSO_3CF_3$ (a) before and (b) after the addition of 200 molar equiv of H_2O.

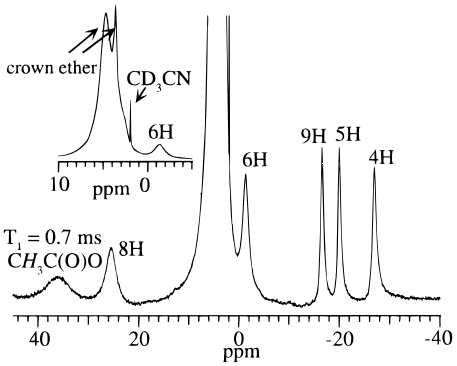

Figure 6. ^{1}H NMR spectrum of [**9b**]OAc·$BaTf_2$·$2H_2O$ in CD_3CN with diamagnetic suppression applied. The resonance at 38 ppm is from the C*H*$_3$ group of the [C*H*$_3$CO(O)]$^-$ bound to Mn(III).

resonances for [**9b**]$^+$·Na^+ suggests that the Na^+ feels the magnetic field of the Mn(III) possibly in both a dipolar sense and a contact term; the contact term arises from the simultaneous binding of Na^+ and Mn(III) to the phenolic oxygens.

The ^{1}H NMR spectrum of [**9b**]OAc·$BaTf_2$·$2H_2O$ (Figure 6 and Table 4) in CD_3CN is different from the spectrum of [**9b**]$^+$·Ba^{2+} in CD_3CN. [**9b**]OAc·$BaTf_2$·$2H_2O$ has a broad resonance at 36 ppm that is absent in [**9b**]$^+$·Ba^{2+}, and no resonance for a H_2O or OH^- bound to the Mn(III) center is observed at 17 ppm (Table 4). A resonance from a bound water molecule could be broadened beyond our detection limits or masked by crown ether resonances. The resonance at 36 ppm for [**9b**]OAc·$BaTf_2$·$2H_2O$ arises from the CH_3 group of the bound acetate. This was shown by adding $CD_3CO(O)D$ to a CD_3CN solution of this complex, which caused the loss of the 36 ppm resonance and concurrent appearance of a signal at 2.1 ppm for free [C*H*$_3$C(O)O]$^-$. Furthermore, the resonance at 36 ppm was absent when [**9b**]OAc was prepared using $Mn(CD_3C(O)O)_2$. In the related compound $[Mn^{III}(\mu\text{-}O)(O_2CCH_3)_2(HB(pz)_3)_2]$ ($HB(pz)_3^-$ = hydrotris(1-pyrazolyl)borate), the methyl group of the bridging acetate ligand has a chemical shift of +65.6 ppm.[58] In addition to the large downfield shift of the acetate CH_3 group in [**9b**]OAc·$BaTf_2$·$2H_2O$, its rapid T_{1p} value, 0.7 ms, indicates that the paramagnetic nature of the Mn(III) center is projected strongly through the carboxylate group.

All of the salt complexes prepared using [**9b**]OAc as a starting material exhibit spectra consistent with acetate binding to Mn(III) (Table 4). The chemical shift of the acetate CH_3 group depends on which cation is in the crown ether. This effect may arise from different degrees of acetate binding in a bridging mode to the cation in the crown ether. The variability of acetate binding/bridging is, in turn, likely to influence both the contact and dipolar shifts arising from the Mn(III) center and thus the chemical shift of the methyl group. We are in the process of preparing crystalline forms of some of the cation-containing compounds to determine crystallographically how acetate binding depends on the cation in the crown ether.

Axial Ligation to [LMn(III)]$^+$ Monomers. Since we could observe differences in the type of axial ligands bound to the Mn(III) in [**9b**]OAc·$BaTf_2$·$2H_2O$ and [**9b**]$^+$·Ba^{2+} by ^{1}H NMR spectroscopy, we examined axial ligation to other monomers prepared in this study. It is well-known that Mn(III) porphyrin and Schiff-base complexes bind one or two axial ligands.[59−61] The binding constants and other thermochemical parameters for some of these binding events have been determined, but these parameters do not assess either how the Mn(III) center perturbs the axial ligand or how the axial ligand might affect properties of the chelate ligand. With regard to photosystem II, it is significant to ascertain how water molecules in particular interact with the various sites of the tetramanganese cluster. In a recent publication,[62] ENDOR and ESEEM data have been used to observe the binding of water and methanol to the Mn^{III} center of a Mn^{III},Mn^{IV} dimer.[63] The very interesting result from that study is that the hydrogens of the bound water molecule are at different distances from the Mn^{III} center. ^{1}H NMR spectroscopy can be an important tool for providing complimentary data regarding water binding to Mn(III) centers.

We have found that **[6b]**$^+$ is an especially valuable complex for observing axial ligand binding to Mn(III) by multinuclear NMR spectroscopy. The discussion that follows pertains to [**6b**]$^+$ unless otherwise noted. Solvated monomers of [**6b**]$^+$ prepared by the CH_3OH/O_2 and $CH_3CN/[Cp_2Fe]^+$ oxidation methods produced compounds with different axial ligands. The differences are readily apparent when the compounds are examined by ^{1}H NMR spectroscopy in CD_3CN. Other analytical methods (electrochemistry, FT-IR, and UV/Vis spectroscopy) that we applied to the characterization of [**6b**]$^+$ that had been prepared by the two oxidation methods erroneously led us to believe that the two oxidation methods produced identical compounds. Shown in Figure 7a is the spectrum of [**6b**]$^+$ prepared by the CH_3OH/O_2 oxidation method while Figure 7b is the spectrum of [**6b**]$^+$ synthesized by the alternative oxidation method. The broad, rapidly relaxing (T_{1p} = 0.7 ms) resonance at 16 ppm in Figure 7a arises from the CH_3 group of a CH_3OH molecule bound to Mn(III) as this resonance is lost upon the addition of CD_3OD; this compound is designated as [**6b**]$^+$·CH_3OH. For the compound used to obtain the spectrum in Figure 7b, we assume that CH_3CN is the axial ligand prior to dissolution in CD_3CN, but that it is rapidly replaced by CD_3CN; this complex is referred to as [**6b**]$^+$·CH_3CN. [**6b**]$^+$·CH_3CN is not sufficiently soluble in CH_2Cl_2 to permit determining the chemical shift of the bound CH_3CN. Comparison of the resonance positions for the Schiff-base ligand hydrogens on [**6b**]$^+$·CH_3OH and [**6b**]$^+$·CH_3CN reveals that they are only slightly influenced by the axial ligand. A similar observation has been made for Mn(III) Schiff-base compounds with alkane backbones.[11]

X-ray quality single crystals of [**6b**]$^+$ were obtained by dissolving a sample of [**6b**]$^+$·CH_3OH in CH_3CN without

(58) Sheats, J. E.; Czernuszewicz, R. S.; Dismukes, G. C.; Rheingold, A. L.; Petrouleas, V.; Stubbe, J.; Armstrong, W. H.; Beer, R. H.; Lippard, S. J. *J. Am. Chem. Soc.* **1987**, *109*, 1435.
(59) Collman, J. P.; Brauman, J. I.; Hampton, P. D.; Tanaka, H.; Bohle, D. S.; Hembre, R. T. *J. Am. Chem. Soc.* **1990**, *112*, 7980.
(60) Hill, C. L.; Williamson, M. M. *Inorg. Chem.* **1985**, *24*, 2836.
(61) Collman, J. P.; Lee, V. J.; Keller-Yuen, C. J.; Zhang, X.; Ibers, J. A.; Brauman, J. I. *J. Am. Chem. Soc.* **1995**, *117*, 692.
(62) Randall, D. W.; Gelasco, A.; Caudle, M. T.; Pecoraro, V. L.; Britt, R. D. *J. Am. Chem. Soc.* **1997**, *119*, 4481.
(63) Larson, E.; Haddy, A.; Kirk, M. L.; Sands, R. H.; Hatfield, W. E.; Pecoraro, V. L. *J. Am. Chem. Soc.* **1992**, *114*, 6263.

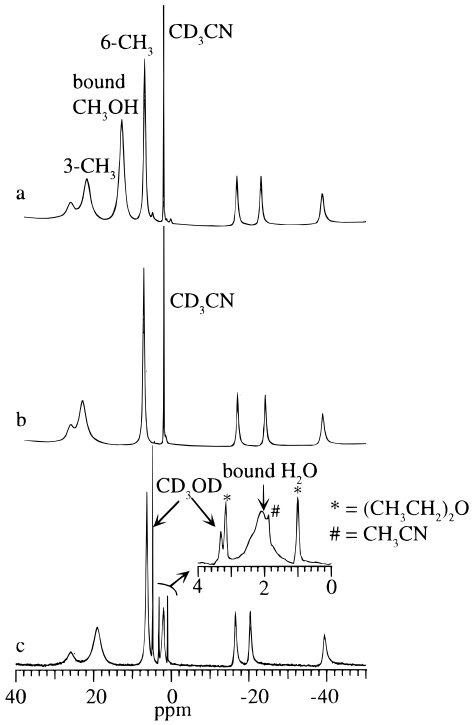

Figure 7. ^{1}H NMR spectra with diamagnetic suppression applied, of (a) [**6b**]$^+$·CH_3OH in CD_3CN, (b) [**6b**]$^+$·CH_3CN in CD_3CN, and (c) [**6b**]-PF_6·H_2O in CD_3OD. The inset in part c highlights the spectral region containing the resonance tentatively assigned as a H_2O molecule strongly bound to the Mn(III) center. Peaks for CH_3CN and $(CH_3CH_2)_2O$ respectively, are from the crystallization process.

Table 5. Selected Bond Lengths (Å) and Angles (deg) for [**6b**]PF_6·H_2O

Mn1−O1	1.863(7)	P1−F2	1.52(1)
Mn1−O3	2.217(8)	P1−F4	1.463(9)
Mn1−N2	1.959(8)	P1−F6	1.54(1)
Mn1−O2	1.836(7)	P1−F1	1.52(1)
Mn1−N1	1.997(8)	P1−F3	1.51(1)
O3−F1	3.01(1)	P1−F5	1.46(1)
O1−Mn1−O3	100.8(3)	F1−P1−F2	174.4(7)
O2−Mn1−O3	88.4(4)	F3−P1−F5	177(1)
O3−Mn1−N1	92.2(4)	F4−P1−F6	177.2(8)
O3−Mn1−N−2	94.7(4)		

excluding air and then allowing the diffusion of Et_2O vapor into the CH_3CN solution. The molecular structure is shown in Figure 8a. Data pertinent to the structure can be found in Table 2 while selected bond distances and angles are given in Table 5. The Mn(III) center resides in an essentially square pyramidal environment with the equatorial plane defined by the Schiff-base ligand and the axial site occupied by a water molecule, Mn1−O3 2.217(8) Å. We refer to this molecule as [**6b**]-PF_6·H_2O. Mn^{III}−O and Mn^{III}−N distances to the Schiff-base ligand are similar to those found in other five- and six-coordinate Schiff-base complexes. The bound water molecule in [**6b**]-PF_6·H_2O is particularly interesting because of the hydrogen-bonding interaction with F1, O3−F1 3.01 Å. Hydrogen bonding to PF_6^- is rare, and we have found only a few recent examples of transition metal aqua complexes with hydrogen bonds to PF_6^- in the solid state.[64,65] As discussed below, the hydrogen bond in [**6b**]PF_6·H_2O persists in CD_3OD. Identification of the hydrogen bond in [**6b**]PF_6·H_2O is significant because F^- is an

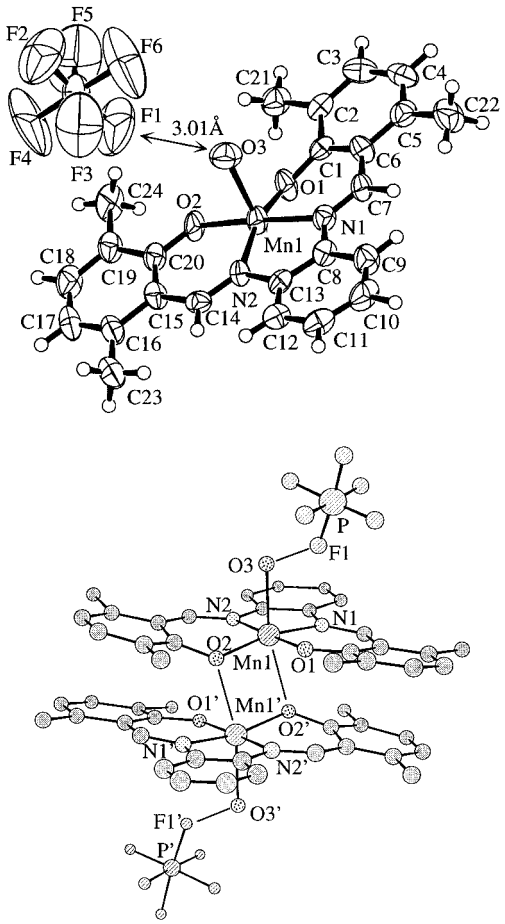

Figure 8. (a, top) ORTEP diagram and atom-labeling scheme for [**6b**]-PF_6·H_2O. Ellipsoids correspond to 50% probability. (b, bottom) A schematic view of [**6b**]PF_6·H_2O that emphasizes the Mn1−O3−F1 interaction and the association of O2 with Mn1 on a neighboring compound.

inhibitor of the catalase enzyme[66] and it is proposed that a water molecule bound to the manganese dimer is hydrogen bonded to the fluoride anion. Despite the hydrogen bond to F1 in [**6b**]-PF_6·H_2O, the bond distances and angles in the PF_6^- are not significantly distorted (Table 5). There is a weak contact between the second axial site on the Mn1 and a phenol oxygen from a neighboring complex, Mn1−O2′ 2.780(8) Å. This contact slightly distorts the square plane of the ligand; this is shown schematically in Figure 8b. We believe that this is the type of interaction that occurs in the dried monomers.

Shown in Figures 9, traces a and b, are FT-IR spectra of [**6b**]-PF_6·H_2O and [**6b**]$^+$·CH_3OH, respectively. It is evident in the spectrum of [**6b**]PF_6·H_2O that the bands at 842 and 558 cm^{-1} characteristic of free PF_6^- are absent. If [**6b**]$^+$·CH_3OH was recrystallized from CH_3CN/Et_2O in an inert atmosphere glovebox using dried solvents (<5 ppm H_2O), the precipitate was a finely divided powder that exhibited absorption bands characteristic of free PF_6^-. The addition of two drops of H_2O (approximately 0.2 mL) to another sample of [**6b**]PF_6 in CH_3CN under the same inert atmosphere conditions produced crystalline [**6b**]PF_6·H_2O. Clearly, hydrogen bonding to the PF_6^- is essential for the formation of X-ray quality single crystals of this molecule, and there must be a strong driving force for binding water to the Mn(III) center.

Compound [**6b**]PF_6·H_2O is insoluble in CH_3CN while [**6b**]$^+$·CH_3OH is freely soluble in that solvent. Both compounds are

(64) Colquhoun, H. M.; Doughty, S. M.; Maud, J. M.; Stoddart, J. F.; Williams, D. J.; Wolstenholme, J. B. *Isr. J. Chem.* **1985**, *25*, 15.
(65) Sletten, J. *Acta Chem. Scand. Ser. A* **1983**, *37*, 569.
(66) Penner-Hahn, J. E. In *Structural Properties of the Manganese Site in the Manganese Catalases*; Penner-Hahn, J. E., Ed.; VCH Publishers: New York, 1992; p 29.

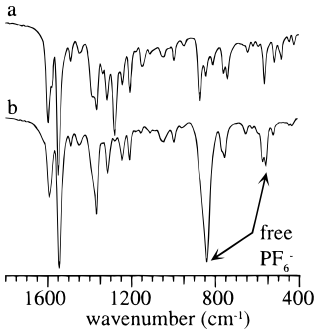

Figure 9. FTIR spectra of (a) [**6b**]PF_6·H_2O and (b) [**6b**]$^+$·CH_3OH as KBr disks.

soluble in CH_3OH. The ^1H NMR spectrum of [**6b**]PF_6·H_2O in CD_3OD exhibits a broad, rapidly relaxing signal at 2.1 ppm which we tentatively assign to the axially bound H_2O molecule in addition to the resonances expected for the ligand (Figure 7c). We expected that either CD_3OD would exchange with the bound water molecule or an H/D exchange of the protons on this H_2O molecule would occur, resulting in a spectrum resembling the one for [**6b**]$^+$·CH_3OH in CD_3OD. However, the continued observation of the bound water signal in the spectrum of [**6b**]PF_6·H_2O suggested that CD_3OD did not displace the water. In addition, the resonance position of the bound water also was at abnormally high fields compared to the other Mn(III) compounds we have investigated. The lack of H/D exchange is especially interesting as the water is bound to a cationic metal center which should render it rather acidic.[67] We speculated that the unusual properties of the bound water molecule observed in the ^1H NMR spectrum arose from the hydrogen bond to the PF_6^- remaining intact in CD_3OD. This hypothesis was tested by acquiring the ^{19}F NMR spectra of [**6b**]-PF_6·H_2O and [**6b**]$^+$·CH_3OH in CD_3OD.

The ^{19}F NMR spectrum of [**6b**]$^+$·CH_3OH in CD_3OD has a doublet for the PF_6^- counterion centered at 40.3 ppm (J_{P-F} 710 Hz) as shown in Figure 10a; a spectrum of KPF_6 in CD_3OD has a doublet at 41 ppm (J_{P-F} 706 Hz). In contrast, [**6b**]PF_6·H_2O in CD_3OD has a broader upfield-shifted doublet centered at 32.5 ppm (J_{P-F} 980 Hz) and only a trace of free PF_6^- (Figure 10c). We estimate that the concentration of free PF_6^- in solution for [**6b**]PF_6·H_2O is on the order of 500 times lower than the concentration of the hydrogen-bonded PF_6^- in this sample. It was substantially more difficult to obtain the ^{19}F NMR spectrum of [**6b**]PF_6·H_2O than to obtain that of [**6b**]$^+$·CH_3OH. The spectrum shown in Figure 10c is the result of approximately 20 h of data collection whereas only 20 min was needed for the one in Figure 10a; the concentrations of [**6b**]PF_6·H_2O and [**6b**]$^+$·CH_3OH were 0.033 and 0.036 M, respectively, in these experiments. The difficulty in observing the ^{19}F signal for [**6b**]-PF_6·H_2O indicated that the PF_6^- strongly experienced the magnetic field of the Mn(III) center. The ^1H and ^{19}F NMR data taken together are consistent with preservation of the hydrogen bond between the Mn(III)-bound water and its PF_6^- counterion as observed in the solid state data for [**6b**]PF_6·H_2O.

Instead of one doublet for the hydrogen-bonded PF_6^- counterion in the ^{19}F NMR spectrum of [**6b**]PF_6·H_2O, we expected to observe three resonances, all with ^{31}P and ^{19}F coupling, because the PF_6^- has its symmetry lowered to C_{4v} by the hydrogen bond. There are at least three explanations which might account for the observed spectral doublet. First, the doublet may arise from an average structure for the anion in solution where each fluorine resides for only a short time on the water hydrogens. This may be pictured as an arrangement in which the PF_6^- tumbles on the bound water molecule. The second possibility is that only one of the axial fluorines, probably the one *trans* to the hydrogen bond, or all of the equatorial fluorines give rise to the doublet, and there is weak or no F−F coupling. The third explanation is that the signal arises from a species other than [**6b**]PF_6·H_2O but one that also has the PF_6 associated with the Mn(III) center. We believe that the second explanation is the most correct one. If the *trans* fluorine is the origin of this resonance, then one would expect that the signal intensity should be, at best, $^1/_6$ that of an unbound PF_6^-. From signal to noise considerations one would expect that a 36-fold increase in the acquisition time would be required, which is in good agreement with our observations. When the influence of the magnetic field from the Mn(III) is included, this would further diminish the predictions for signal intensity. In view of the long acquisition times required to obtain spectra of [**6b**]-PF_6·H_2O (20 h), variable temperature studies have not been initiated which could be a means to distinguish the three possible explanations or suggest others.

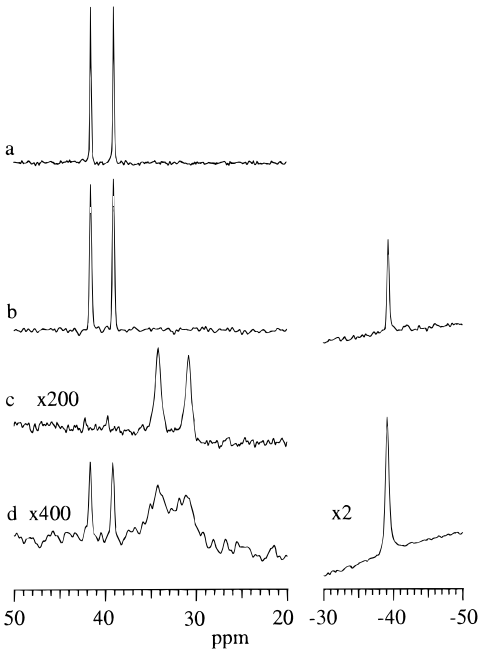

Figure 10. ^{19}F NMR spectra in CD_3OD of (a) [**6b**]$^+$·CH_3OH, (b) [**6b**]$^+$·CH_3OH containing 0.5 molar equiv of (n-Bu_4N)BF_4, (c) [**6b**]-PF_6·H_2O, and (d) [**6b**]PF_6·H_2O containing 0.5 molar equiv of (n-Bu_4N)-BF_4.

It was of interest to determine if the hydrogen-bonded PF_6^- could undergo exchange reactions with BF_4^-. For this experiment, 0.5 molar equiv of (n-Bu_4N)BF_4 was added to a solution of [**6b**]$^+$·CH_3OH in CD_3OD and the ^{19}F NMR spectrum obtained, Figure 10b; the ^{19}F NMR spectrum of (n-Bu_4N)BF_4 alone appears as a singlet at −39.2 ppm in CD_3OD. There are no differences in the spectrum when compared to the one in Figure 10a. In contrast, clear changes occurred when 0.5 molar equiv of (n-Bu_4N)BF_4 was added to [**6b**]PF_6·H_2O in CD_3OD. It can be seen in Figure 10d that the signal associated with the bound PF_6^- decreased in intensity and broadened compared to the one in Figure 10c, while the doublet for the free PF_6^- increased in intensity by a factor of about 10. The concentration of "free" PF_6^- was still about 50 times lower than the amount of bound PF_6^- at 8 h after the addition of BF_4^-, as determined by integration of the "free" PF_6^- signals. The peak width at half-height for the signal from the BF_4^- was approximately twice as large as it is in Figure 10b, indicating that BF_4^- can hydrogen bond to the Mn(III)-bound water molecule. In view

(67) Cotton, F. A.; Wilkinson, G. *Advanced Inorganic Chemistry*, 5th ed.; J. Wiley & Sons: New York, 1988.

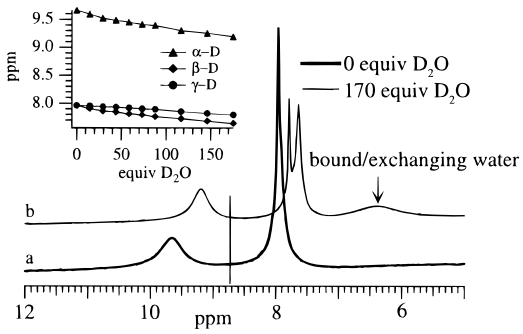

Figure 11. ^{1}H NMR spectra of a dried sample of $[\mathbf{1b}]^+$ dissolved in py-*d* containing (a) 0 and (b) approximately 170 equiv of added D_2O; the vertical line at 8.74 ppm indicates the chemical shift for the α-hydrogens of free pyridine. The graphical insert depicts the change in chemical shift of the pyridine hydrogens as a function of the amount of D_2O added to the sample.

of the extremely long acquisition times required for examining the reaction of $[\mathbf{6b}]PF_6{\cdot}H_2O$ with BF_4^-, we have not attempted to measure the equilibrium constant for the PF_6^-/BF_4^- exchange.

The results of the NMR experiments described above illustrate some rather interesting properties of $[\mathbf{6b}]^+$. First, $[\mathbf{6b}]^+$ can be prepared with three different axial ligands, each of which has characteristic NMR properties. In this context, the ^{19}F NMR data were important for correcting our initial interpretation of the IR data for $[\mathbf{6b}]PF_6{\cdot}H_2O$ where we thought that PF_6^- was absent (Figure 9). Second, the precipitation of $[\mathbf{6b}]PF_6{\cdot}H_2O$ from solution must be the driving force for formation of this compound because the deliberate addition of water (0.5−4 equiv) to $[\mathbf{6b}]^+{\cdot}CH_3OH$ in CD_3CN does not produce $[\mathbf{6b}]$-$PF_6{\cdot}H_2O$ within 24 h, as determined by ^{1}H NMR measurements. Third, the water molecule appears to remain coordinated to the Mn(III) center during the BF_4^-/PF_6^- exchange. Finally, it was anticipated that BF_4^- would displace the hydrogen-bonded PF_6^- as it has a less diffuse charge. However, the results suggest that PF_6^- binding is favored under the current reaction conditions.

Pyridine Coordination. The final axial ligand examined was pyridine-d_5, py-*d*. Pyridine is often used as an axial ligand for planar Mn(II) and Mn(III) compounds, and equilibrium binding constants have been obtained for Mn(II) and Mn(III) porphyrin complexes.[59−61,68] In the case of the Mn(III) porphyrins, both five- and six-coordinate complexes are observed. Electrochemical data for some Mn(III) Schiff-base compounds examined in our laboratory[16] indicated that pyridine and *N*-methylimidazole were axial ligands for Mn(III) centers; in particular, $Mn^{III/II}$ couples shifted cathodically and O_2 binding rates for Mn(II) compounds changed upon inclusion of these axial ligands. We wished to ascertain if pyridine binding was observable by NMR spectroscopy. A similar NMR study has previously been performed on Mn(III) porphyrins,[60] but the results here are somewhat different because water competes with pyridine for binding to the Mn(III) center in the Schiff-base complexes.

The NMR samples for these experiments were prepared by dissolving $[\mathbf{1b}]^+$ (dried form) in py-*d* from a freshly opened ampule in an inert atmosphere glovebox to ensure the driest possible conditions. The ^{1}H NMR spectrum of $[\mathbf{1b}]^+$ prepared under these conditions exhibited two resonances at 9.64 and 7.96 ppm in addition to those arising from the ligand (Figure 11a; for purposes of clarity, ligand resonances are not included, but they correspond closely to those shown in Figure 2). The asymmetry of the upfield peak suggested that it was composed of at least two resonances. Py-*d* in the absence of $[\mathbf{1b}]^+$ has resonances at 8.74 (α-H; vertical line in the figure), 7.58 (γ-H), and 7.22 (β-H) ppm. Clearly there are no resonances for "free" py-*d* in the spectrum (a capillary containing acetone was placed in the NMR tube to serve as the chemical shift standard). On the basis of a proximity argument, we presume that the most downfield resonance arises from the α-hydrogen and the other resonance is from the γ- and β-hydrogens.

^{1}H NMR results for paramagnetic Ni(II) compounds that strongly bind pyridine and Fe(III) dimers[69,70] that irreversibly bind ligands composed of pyridyl groups indicate that the following three features should be observed in the spectrum of $[\mathbf{1b}]^+$ if the py-*d* is bound strongly to the Mn(III) center: (i) chemical shifts for the py-*d* should be 10−100 ppm from those of free py-*d*; (ii) three well-separated py resonances should be present; and (iii) the chemical shift for the β-hydrogen should be downfield of the γ-hydrogen. Since none of these three conditions were observed here, we concluded that the py-*d* was undergoing an exchange process at the Mn(III) center that was rapid on the NMR time scale and that the β- and γ-hydrogens gave rise to the upfield resonance. The rapid exchange process is not surprising because axial ligands on Mn(III) centers in square planar complexes are generally labile and the concentration of $[\mathbf{1b}]^+$ (38.9 mM) is low relative to that of pyridine (12.5 M).

As noted above, dry conditions had to be used to prepare the samples in py-*d* because water competes effectively with py-*d* for binding to the Mn(III) center. Shown in Figure 11b is the spectrum taken after 170 equiv of D_2O had been added to the solution used to obtain the spectrum in Figure 11a. There are now three resonances for the py-*d* (9.19, 7.79, and 7.64 ppm), and a broad peak for water appears at 6.37 ppm; free water in py-*d* is at ∼5 ppm. The insert in Figure 11 is a plot of the chemical shift for the py-*d* resonances *vs* quantity of D_2O added. The significant points regarding the plot are (i) the change in chemical shift for the py-*d* resonances is not a linear function of D_2O added; (ii) all of the py-*d* resonances shift upfield as a consequence of the D_2O addition, but even after 170 equiv (6.67 M) of D_2O have been added, the chemical shifts are not those of free py-*d*; and (iii) each resonance exhibits a different rate of upfield shift. The first two points along with the chemical shift value for the water in Figure 11b lead us to conclude that there is an equilibrium between water and py binding to the Mn(III) center. Equilibria such as those in eq 4 are likely, and we are in the process of evaluating the relative binding affinities of $[\mathbf{1b}]^+$ for water and py. Regarding the third point, it can be

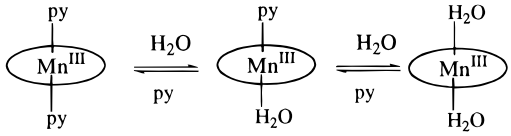

(4)

seen on the plot that the chemical shifts for the two peaks arising from the single upfield resonance in Figure 11a are diverging as the quantity of water increases. This requires that the more downfield member of this pair be due to the γ-hydrogen. Furthermore, if one makes the extrapolation to irreversible binding of the py to Mn(III), then the β-hydrogen would be downfield of the γ-hydrogen as observed for Ni(II) complexes.

It is quite interesting that $[\mathbf{1b}]^+$ is so effective at scavenging even small quantities of water in pyridine; even at 15 equiv of

(68) Collman, J. P.; Brauman, J. I.; Fitzgerald, J. P.; Hampton, P. D.; Naruta, Y.; Michida, T. *Bull. Chem. Soc. Jpn.* **1988**, *61*, 47.

(69) Norman, R. E.; Holz, R. C.; Menage, S.; O'Connor, C. J.; Zhang, J. H.; Que, L., Jr. *Inorg. Chem.* **1990**, *29*, 4629.

(70) Norman, R. E.; Yan, S.; Que, L., Jr.; Backes, G.; Ling, J.; Sanders-Loehr, J.; Zhang, J. H.; O'Connor, C. J. *J. Am. Chem. Soc.* **1990**, *112*, 1554.

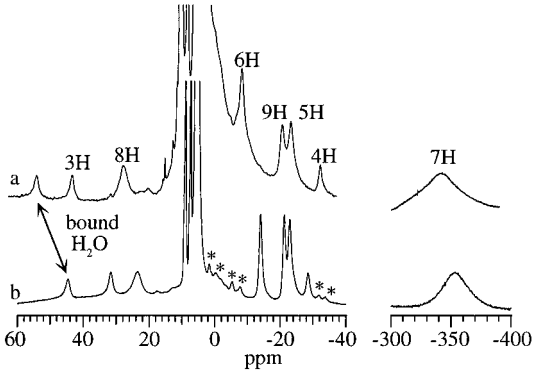

Figure 12. ^{1}H NMR spectra of **1c** in (a) CD_2Cl_2 and (b) py. The resonances marked with an asterisk (*) in part b arise from **1c** having py coordinated to the Mn(III) center(s).

D_2O in the presence of 320 equiv of py-*d*, some displacement of pyridine occurs. This behavior most likely reflects the oxophilic nature of manganese. Furthermore, in almost all of our ^{1}H NMR spectra, the traces of water that are always present even in high-quality NMR solvents are not detected under routine data collection conditions (no diamagnetic suppression applied). Presumably, when the trace water in a given solvent binds to Mn(III), the paramagnetic nature of the metal center broadens the resonance and shifts it far from the chemical shift region being probed. Thus, it appears that all of the Mn(III) monomer compounds used in this study bind water strongly.

Mn^{III}_2 μ-Oxo Dimers. Some general comments about obtaining NMR spectra of the dimers are warranted before presentation of the data. First, the μ-oxo dimers are more difficult to examine than the monomers because of their lower solubility. Only non-hydroxylic solvents can be used because the μ-oxo dimers are cleaved in alcohol solvents. Even some non-hydroxylic solvents, DMF and DMSO, appear to cleave selected μ-oxo dimers, indicating that the Mn−O−Mn functionality has limited stability. Second, from systematic substitution of the ligand hydrogens, we found that the resonance positions for a few of the ligand hydrogens are more variable in the μ-oxo dimers than they are in the monomers. This behavior may arise from both steric interactions and enhanced dipolar effects from an adjacent Mn(III) center. Third, axial ligation to the Mn(III) centers occurs in the μ-oxo dimers, but in the dimers, unlike the monomers, chemical shifts of the ligand hydrogens are strongly affected by the axial ligand. Finally, the solvent can cause shifts of up to 10 ppm upfield or downfield for some resonances. Thus, there are some occasional difficulties in making definitive chemical shift assignments for the μ-oxo dimers. However, owing to the sensitivity of the μ-oxo dimers to the conditions under which the spectrum is obtained and the presence of some signature resonances, one can immediately identify a μ-oxo dimer in the presence of a monomer. The ability to differentiate between these two species was a primary goal of the NMR study.

The spectrum of $[(SALOPHEN)Mn^{III}]_2(\mu\text{-O})$, **1c**, in CD_2Cl_2 displays eight resonances (Figure 12a and Table 4), which is one more resonance than for $[\mathbf{1b}]^+$ in CD_3OD. The spectrum of each of the dimers synthesized in either CH_2Cl_2 or CH_3CN showed one extra resonance as compared to the spectrum of its corresponding monomer. Seven resonances are expected for a μ-oxo dimer composed of square planar SALOPHEN ligands adopting a cofacial or bent arrangement and maintaining roughly C_{2v} or C_s symmetry. Fourteen resonances might be observed for a distorted ligand structure, but the ^{1}H NMR spectra of other distorted Mn(III) Schiff-base complexes[10,12,13] show fewer resonances. Since the spectrum of **1c** has only one additional resonance and the pattern of four upfield and three downfield resonances, plus the one extra, is preserved, we assume that the ligand is essentially square planar in the μ-oxo dimer. From an approach involving the systematic substitution of ligand hydrogens, the most downfield resonance, which occurs at 51.4 ppm in Figure 12a, was concluded to be the additional one; of particular importance was the observation that this resonance did not arise from a hydrogen on the Schiff-base ligand. Indicated on the figure are the resonance assignments based on a substitution matrix similar to the one used in determining the resonance assignments given in Figure 2b. Since the additional resonance in the spectrum of the μ-oxo dimer was not from the Schiff-base ligand and it has a rapid relaxation rate, it must be an axial ligand on Mn(III). In view of the synthetic protocol used to produce the μ-oxo dimers, two likely candidates for the putative axial ligand were methanol and water.

Our initial thought was that a water or methanol molecule was introduced during the synthesis of the Mn(II) starting material (see above) and that, following the oxygenation reaction, the methanol or water remained bound to the Mn(III) center. In order to test this hypothesis, $(SALOPHEN)Mn^{II}$ was synthesized in CD_3OD; the resulting solid was washed with D_2O, dried under vacuum, and then oxygenated in CD_2Cl_2 to produce **1c**. The ^{1}H NMR spectrum of this material showed the resonance at 51.4 ppm to be of the same intensity relative to 8H as a sample of **1c** prepared using **1a** synthesized in CH_3OH and washed with H_2O. This experiment eliminated methanol or water as an axial ligand being introduced at the Mn(II) stage. We surmised then that the axial ligand was water that becomes bound during the oxygenation process.

That the downfield resonance was due to bound water was confirmed by obtaining the spectrum of **1c** in py-*d* (δ = 44.7 ppm for the downfield resonance in py-*d*). We assumed that py-*d* would displace some or all of the bound water resulting in loss of the downfield resonance; the released water ligand then could be conclusively identified from its chemical shift. The spectrum of a sample of **1c** prepared under Ar and taken within 20 min of being dissolved in py-*d* is shown in Figure 12b. We have interpreted the peaks marked with an asterisk (*) as arising from the small portion of μ-oxo dimer molecules that become coordinated by py-*d*. We were somewhat surprised to find that the concentration of py-coordinated dimer increased only very slowly. However, our studies using the Mn(III) monomers described above indicated that water binds strongly to Mn(III) centers.

Slow loss of the bound H_2O was confirmed by allowing the sample to stand in the py-*d* and acquiring spectra periodically over 3 weeks. The NMR tube was maintained under Ar between runs. Selected spectra are shown in Figure 13. It is clear that the resonance at 44.7 ppm decreased in intensity during the experiment while one at 5 ppm for free H_2O in py-*d* increased. A plot of the normalized increase in signal intensity for water released and the normalized decrease in the signal at 44.7 ppm *vs* time is shown as an inset in Figure 13. This result indicates that the free water comes from the species responsible for the resonance at 44.7 ppm. As there is little change after 14 days, the reaction appears to reach equilibrium by that time.

The complicated nature of the spectrum taken after 14 days is consistent with multiple species. First note that there is no $[\mathbf{1b}]^+(py)(H_2O)$ (compare with Figure 11) so decomposition of the dimer did not appear to occur to any significant extent. We believe that there are three species in solution: $Mn^{III}_2(\mu\text{-O})(H_2O)_2$, $Mn^{III}_2(\mu\text{-O})(H_2O)$(py-*d*), and $Mn^{III}_2(\mu\text{-O})$(py-*d*)$_2$. No attempt has been made to assign the resonances arising from the latter two compounds.

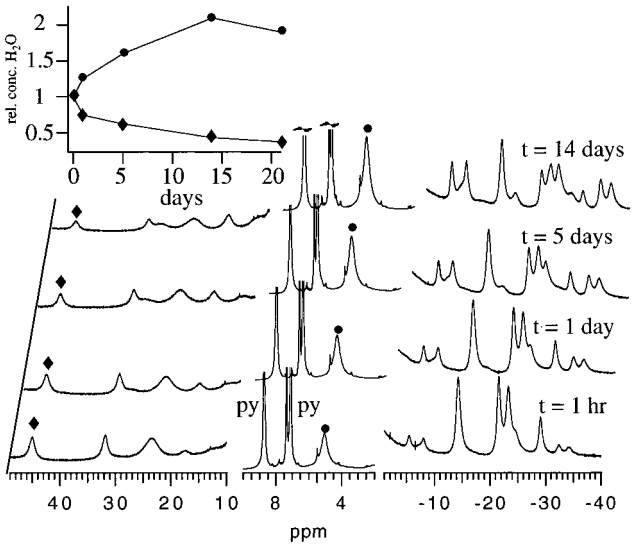

Figure 13. ^{1}H NMR spectra of **1c** in py-*d* obtained at the times indicated on the figure. The resonances denoted with the symbol ♦ arise from H_2O bound to Mn(III) while those marked with the symbol ● are for free H_2O in py. The inset shows the changes in normalized signal intensities for bound and free H_2O as a function of time.

The NMR data suggest that the μ-oxo dimers have essentially the same square planar ligand geometry observed for the monomer and that the overall symmetry of the dimer is C_s or C_{2v}. At least two options are available for the orientation of the ligands: *trans* (**VI**) or *cis* (**VII**) orientation of aromatic rings. In view of the steric demands of the *tert*-butyl groups on **8c**, we suggest that **VI** is a better description than **VII**. The

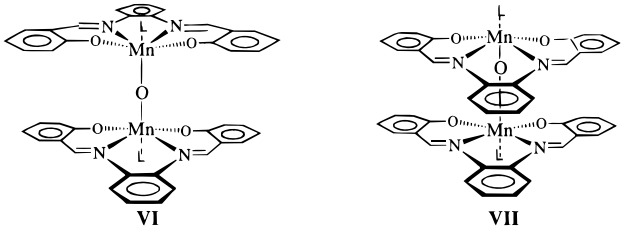

VI **VII**

proposed structure is similar to ones observed in solid state structures of oxo-bridged Ti(IV)[71] and Fe(III)[72−76] Schiff-base complexes although some V^V═O Schiff-base dimers do exhibit the *cis*-ligand orientation.[57,77] The available data do not allow us to determine if the Mn(III)−O−Mn(III) unit is linear or bent or if the manganese centers reside within the plane defined by the Schiff-base ligand. However, six-coordinate Mn(III) compounds tend to have the metal center in the plane of the ligand.

Conclusions. ^{1}H NMR spectroscopy is clearly a powerful method to characterize paramagnetic Mn(III) coordination compounds. Its utility is greatly enhanced when it is coupled with a simple diamagnetic suppression routine that reduces the intensity of solvent peaks. Through the application of the diamagnetic suppression routine, it was possible to identify and assign all of the peaks in most of the spectra of the Schiff-base compounds examined in this study. Diamagnetic suppression was particularly useful for those compounds in which a ligand resonance would be masked by a more intense solvent resonance if suppression was not used.

The suppression routine also was a valuable component in revealing the subtleties of axial ligation in these compounds. While many previous workers have shown that axial ligation to Mn(III) coordination complexes is an integral part of the chemistry of these species, the variety of molecules that bind strongly to the Mn(III) centers in our Schiff-base complexes was somewhat surprising. The probing of axial ligation proved to be an effective means for detecting subtle differences in what appeared to be, by other spectroscopic methods, identical compounds. It also revealed the strong, persistent hydrogen bond of a Mn(III)-bound water molecule in [**6b**]PF_6·H_2O to PF_6^-, an anion generally considered to be noncoordinating. As noted above, the ability to observe this hydrogen-bonded species by ^{19}F NMR supports the hypothesis that inhibition of the catalase reaction by F^- may be due to a hydrogen bond between a Mn-bound water molecule and fluoride.

This NMR study also suggested several reasons why we have had difficulty in obtaining single crystals of μ-oxo dimers. In coordinating solvents like py, the existence of multiple species undoubtedly compromises the ability to grow single crystals of a pure compound. While only a single species appears to exist in a noncoordinating solvent like CH_2Cl_2, the very low solubility of the μ-oxo dimer in this solvent generally results in too rapid precipitation and consequently formation of powdery materials.

Finally, the NMR results for the [**9b**]$^+$·M^{n+} complexes are intriguing because a Ca^{2+} cation resides near the tetramanganese core of the OEC, but the function of the Ca^{2+} in the water oxidation process is still a matter of debate. We have shown that cations within approximately 3.5 Å of the Mn^{III}_2 μ-oxo core in the crown ether complex cause substantial anodic shifts in the redox potentials of the dimers.[21] Similar effects are also observed for Mn^{IV}_2 bis(μ-oxo) dimers that incorporate cations. Our NMR and electrochemical results taken together suggest that Ca^{2+} may serve at least two functions in the OEC: (i) enhancing water binding to manganese and (ii) increasing the oxidizing power of the manganese cluster. Even in the absence of Ca^{2+} the affinity of the Mn(III) Schiff-base monomers and dimers for water is much larger than one might have anticipated. Thus, when examining the reaction chemistry of Mn(III) compounds, one must be prepared to at least consider that water will be involved in the reaction of interest.

Acknowledgment. This work was supported by the NSF (CHE 9496236 to C.P.H.).

Supporting Information Available: Tables listing detailed crystallographic data, atomic positional parameters, and bond lengths and angles for [**9b**]OAc·$BaTf_2$·$2H_2O$ and [**6b**]PF_6·H_2O and Figure S1, depicting a matrix of ligand substitutions and assignments of hydrogen resonances (8 pages). Ordering information is given on any current masthead page.

IC970747Z

(71) Sasaki, C.; Nakajima, K.; Kojima, M.; Fujita, J. *Bull. Chem. Soc. Jpn.* **1991**, *64*, 1318.
(72) Marini, K. S.; Murray, K. S.; West, B. O. *J. Chem. Soc., Dalton Trans.* **1983**, 143.
(73) Davies, J. E.; Gatehouse, B. M. *Acta Crystallogr.* **1973**, *B29*, 1934.
(74) Coggon, P.; McPhail, A. T.; Mabbs, F. E.; McLachlan, V. N. *J. Chem. Soc. A* **1971**, 1014.
(75) Gerloch, M.; McKenzie, E. D.; Towl, A. D. C. *J. Chem. Soc. A* **1969**, 2850.
(76) Lewis, J.; Mabbs, F. E.; Richards, A. R. *J. Chem. Soc. A* **1967**, 1699.
(77) Oyaizu, K.; Yamamoto, K.; Yoneda, K.; Tsuchida, E. *Inorg. Chem.* **1996**, *35*, 6634.